Northwest Atlantic Fisheries Organization

Serial No. N6436 **NAFO SCR Doc. 15/015**

SCIENTIFIC COUNCIL MEETING – JUNE 2015

Environmental Conditions in the Labrador Sea during 2014

I. Yashayaev, E.J.H. Head, K. Azetsu-Scott, M. Ringuette, Z. Wang, J. Anning and S. Punshon

Department of Fisheries and Oceans, Maritimes Region
Ocean and Ecosystem Sciences Division, Bedford Institute of Oceanography
P.O. Box 1006, Dartmouth, N.S. B2Y 4A2

Abstract

The Dec-Jan-Feb (DJF) composite North Atlantic Oscillation (NAO) index was strongly positive in 2014 and similar to that of 2012 which was the highest since the mid-1990s. During the winter convection season, the NCEP reanalysis of surface air temperature indicated above normal temperature conditions with a positive anomaly ranging between 1 – 3°C in the Labrador Sea, while the Sea surface temperature (SST) anomalies showed a mixed SST pattern, with negative and positive anomalies for the same period. Most of the Labrador Shelf ice concentration was above normal in the winter months of 2014 (reference period: 1979-2000); however, in the northern part of the Labrador Sea, the sea ice concentration was ~25% below normal in January, and interestingly, the same region had ~25% above the normal ice concentration in March. Wintertime convection in 2014 reached 1600 m, and based on some Argo profiles possibly even 1800 m, which is significantly deeper than the 1000 m seen in the previous year. The deeper part of the intermediate layer (1800-2500 m) of the central Labrador Sea has been gradually warming since the mid-1990s. DIC and pH are following their usual inverted pattern yielding a sustained decline rate in pH of 0.0032 per year since 1996. Silicate concentration in the newly ventilated layer is also decreasing, following the same trend as has been observed in the rest of the North-western Atlantic. Winter conditions and deep convection delayed the phytoplankton bloom by almost a month with a cascading effect on the lower trophic levels thus delaying production by *Calanus finmarchicus* and most of the mezooplankton taxa with all taxa exhibiting lower abundance than normal. In May, the *Calanus finmarchicus* community was still exhibiting the characteristic of a population slowly emerging from their overwintering condition.

Introduction

Since 1990, the Ocean and Ecosystem Sciences Division at the Bedford Institute of Oceanography has carried out annual occupations of a hydrographic section across the Labrador Sea (Figure 1) The section was designated as AR7W (Atlantic Repeat Hydrography Line 7 West) in the World Ocean Circulation Experiment (WOCE). Other than traditional physical seawater characteristics (temperature, salinity, density, currents), these surveys also include chemical (e.g., dissolved oxygen, nutrients, chlorofluorocarbons, sulfur hexafluoride, total inorganic carbon, pH) and biological measurements (e.g., bacteria until 2012, phytoplankton and mesozooplankton). The AR7W line is the major component of the Canadian Department of Fisheries and Oceans (DFO) Atlantic Zone Off-shelf Monitoring Program (AZOMP) and the main Canadian contribution to the international Global Climate Observing System (GCOS) and to the (international) Climate Variability (CLIVAR) component of the World Climate Research Programme (WCRP). The section spans approximately 880 km from the 130 m contour on the inshore Labrador shelf to the 125 m contour on the

West Greenland shelf. Sea ice sometimes limits coverage at the ends of the section. DFO also contributes to the international Argo program by deploying floats in the Labrador Sea and managing and processing the Argo data streams. The importance of international Labrador Sea monitoring and AZOMP, in particular was discussed and emphasized in the recent special issue of Progress in Oceanography (Yashayaev et al., 2015; Kieke and Yashayaev et al., 2015). Indeed, the Labrador Sea can viewed as receiving and blending basin, heart and lung of the Atlantic Ocean and Earth's climate (Yashayaev et al., 2015), and the annual AZOMP multidisciplinary survey of the Labrador Sea (primarily AR7W and profiling Argo floats) present invaluable contribution to the ongoing international ocean and climate monitoring and research effort.

Since this transect has been surveyed for more than two decades, the data now exist to make a meaningful examination of multiyear trends. In addition to the near real-time temperature and salinity Argo float data that started to arrive systematically in 2002, the floats collectively draw a large-scale picture of the hydrographic structure and circulation of the Labrador Sea. The hydrographic variables (temperature, salinity, density, dissolved oxygen, etc.) demonstrate seasonal, inter-annual, decadal and longer-term variability, and the variations are largely governed by the changing contributions of several factors including winter heat losses to the atmosphere, heat and salt gained from Atlantic Waters carried northward into the Labrador Sea by the West Greenland Current, freshwater input from ice and melt from the Arctic and Greenland, continental runoff and precipitation. Occasional severe winters lead to strong cooling of the upper layer, and the resulting increases in the surface density cause the water column to mix to great depths. By the end of winter, convective mixing (hence the name of the process – winter convection) may penetrate deeper than 1500 m and in extreme cases deeper than 2000 m. Milder winters lead to lesser heat losses, thus stronger influence of heat and salt passed from the warm and saline Atlantic Waters, and stronger stratification in the subsurface (>200 m) layers. The atmospheric conditions commonly but not fully (entirely) expressed by (associated with) the North Atlantic Oscillation (NAO) index play an important role in setting the deep convection events in the Labrador Sea, which can help explain development of significant long-term hydrographic phenomena in the region. Under the global warming scenarios, the increasing freshwater inputs from Greenland glacier melting and the Arctic also contribute to the hydrographic variations at seasonal, inter-annual and longer time scales. Continuation of the annual oceanographic sampling on the AR7W line and the on-going support of the Argo float array will help to improve and deepen our understanding of the multi-scale processes and variability, providing a more thorough understanding of the role of the Labrador Sea in global climate system as well as of the dominant physical processes in the regional ecosystem.

A sequence of severe winters in the early 1990s led to deep convection that peaked in 1993–1994. Milder atmospheric conditions prevailed in the following years and the upper layers gradually regained their vertical stratification in density and other physical and chemical properties. The trends of increasing temperature and decreasing density established in the upper 1000 m of the Labrador Sea with the cessation of extreme convection of the first pentad of the 1990 were interrupted in the winters of 2000, 2002 and 2008, 2012 and 2014 when deep convection was observed to the depths often approaching and even exceeding 1500 m in the central Labrador Sea.

In 2014, the net surface heat losses of the entire Northwest Atlantic Ocean (sum of latent and sensible heat fluxes, incoming and outgoing short and long wave radiation) integrated over the cooling season exceeded almost all preceding years of the 20th century, with the exception of 2008 (Josey et al 2015). As a result, the 2014 winter convection in the Labrador Sea generally reached 1600 m, but in some areas was measured to 1800 m; this was the second deepest convection since 1995. Existing ship-based and Argo profiles provide only sparse estimates of maximum convection depth.

Atmospheric System

North Atlantic Oscillation

The NAO is an important teleconnection pattern influencing atmospheric processes in the Labrador Sea (Barnston and Livezey, 1987; Hausser et al., 2015). When the North Atlantic Oscillation (NAO) is in its positive phase, low-pressure anomalies over the Icelandic region and throughout the Arctic combined with high-pressure anomalies across the subtropical Atlantic produce stronger-than-average westerlies across the mid-latitudes. During a positive NAO, conditions are colder and drier than average over the northwestern

Atlantic including the Labrador Sea region. Both NAO phases are associated with basin-wide changes in the intensity and location of the North Atlantic jet stream and storm track, and in large-scale modulations of the normal patterns of zonal and meridional heat and moisture transport (Hurrell, 1995), resulting in changes in temperature and precipitation patterns.

The NAO exhibits considerable interseasonal to interdecadal variability, and prolonged periods of both positive and negative phases of the pattern are common, which seem to have more influence on convection in the Labrador Sea than its short-term fluctuations (Yashayaev, 2007). The wintertime NAO also exhibits significant multi-decadal variability (Hurrell, 1995). An upward trend of the NAO index from the 1960s through the 1990s was noted by Visbeck et al (2001), although since the peak in the 1990s there has been a slight downward trend.

More recent studies reveal a pattern of atmospheric circulation complementary to NAO (Hausser et al., 2015), which becomes more prominent in the years of low NAO. Further study and understanding of this phenomenon will help to improve forecasts of atmospheric situations and oceanic conditions.

In 2010, the NAO index was observed to reach a record low (Figure 2), leading to warmer than normal conditions in this region, which was confirmed by Argo data and the AR7W survey. In 2011, the NAO index rebounded from the record low but still remained significantly below the 30-year average (1981-2010). In 2012, however, the NAO index was strongly positive (12 mbar), up to a level comparable to those in early 1990s showing as the highest winter index over the past twenty years. Significant change in the winter NAO index was seen in 2013 with it being a moderate negative year (-3 mbar). In 2014, the NAO index was back to its high positive phase, and it was just slightly lower than the 2012 one, making it the second highest in the last twenty years, leading to colder than normal winter conditions in the region. However, the situation with the Labrador Sea convection generally following strong changes in NAO showed that the winter mixing in 2012 extended to about1400 m, while in 2014 it went significantly deeper, reaching 1800 m and forming a fairly cold and fresh class of Labrador Sea Water.

Surface Air Temperature

The NCEP/NCAR Reanalysis Project is a joint project between the National Centers for Environmental Prediction (NCEP) and the National Center for Atmospheric Research (NCAR). The goal of this joint effort is to produce new atmospheric analyses using historical data (1948 onwards) and as well to produce analyses of the current atmospheric state (Kalnay et al., 1996).

The NCEP reanalysis of surface air temperature indicated above normal conditions with an anomaly ranging between 1and 3°C in the Labrador Sea during winter, with the biggest winter positive anomalies in the northern part of Baffin Bay (>4°C). It was ~1°C below normal for the most of Labrador Sea during spring, with the strongest negative anomaly patch in the central Labrador Sea, approximately 1°C above normal for the summer period in the Labrador Sea and Baffin Bay, and there was positive anomaly of 0 – 2°C during the fall in the Labrador Sea and Baffin Bay, but a below normal air temperature (2°C below normal) in the northern part of the Hudson Bay (Figure 3).

Sea Surface Conditions

Sea Surface Temperature

To ensure consistency with the air temperature, the SST anomalies (Figure 4) are also generated from the NCEP reanalysis. In general, sea surface temperature (SST) anomalies in the Labrador Sea followed the patterns observed in the air temperature except for the winter time: a mixed SST anomaly pattern was present, negative and positive in the Labrador Sea in the winter of 2014, but in Baffin Bay, anomalies of >3°C were seen throughout the region which is consistent with the air temperature during this season, while for other seasons, positive anomalies were the dominant feature as it was in the air temperature. The SST anomalies in spring were more than 2°C below normal. The summer anomalies were 0.5 - 3°C above normal with the smallest anomalies in the central Labrador Sea. The Baffin Bay and northwest of Labrador Sea had > 2.5°C above normal SST in the fall, and the anomalies in the southeast of the Labrador Sea were significantly smaller than those in the Baffin Bay and northwest of Labrador Sea with anomalies of ~0.5°C. Consistently

with the below normal air temperature in the northern Hudson Bay, the SST in the region was more than 2°C below normal.

Sea Ice

The sea ice data are obtained from The U.S. National Snow and Ice Data Center. Most of the Labrador Shelf ice concentration was above normal in the winter months of 2014 (reference period: 1979-2000). But in the northern part of the Labrador Sea, the sea ice concentration was ~25% below normal in January, and interestingly, the same region had ~25% above the normal ice concentration in March (Figure 5).

AR7W Hydrography

Sea ice generally prevents access to the Labrador Shelf before mid-May; notwithstanding this constraint, the annual AR7W surveys normally take place as early in the spring as practical to provide a consistent view of interannual changes resulting from the large seasonal changes in physical, chemical, and biological properties. In addition to the AR7W Line, a full AZOMP survey also includes sampling of the extended Halifax Line (XHL) to monitor variability on the Scotian Rise and Slope in the deep western boundary flows of the North Atlantic and to obtain additional information on oceanographic and lower-trophic-level variability of the Slope Water affecting the Scotian and adjacent shelves (http://www.bio.gc.ca/science/monitoring-monitorage/azomp-pmzao/azomp-pmzao-eng.php). The survey in 2014 was conducted aboard the CCGS Hudson from the 2nd to the 26rd of May (See Figure 1).

Change in temperature and salinity in the upper layers of the Labrador Sea occur in response to changes in: atmospheric forcing, warm and saline inflows via the Irminger Current and shallower fresh and cold via the West Greenland and Labrador Currents, and freshwater inputs originating from precipitation, runoff and glacier melt. Seasonal cycles in each of these three forcing terms drive a strong seasonal cycle in the properties of the upper layers of the Labrador Sea. Significant decadal variability has also been observed in the central Labrador Sea. While there has been relatively little variability below 2500 m, there have been significant decade-long events in the upper 2000 m. A period of warming and increase in salinity during the mid-1960s to mid-1970s was followed with an inverse period of cooling and freshening during the 1990s characterised by deep winter convection that filled the upper two kilometers of the Labrador Sea (in some years it has reached 2400 m and possibly deeper) of the water column with cold and fresh water. Milder winters in recent years have produced more limited amounts of mode waters, which have gradually become warmer, saltier, and less dense than a decade and a half ago. This recent trend changed abruptly during the cold winter of 2008 when deep convection to 1600 m was observed. The environmental conditions that contributed to the 2008 deep convection have been documented by Yashayaev and Loder (2009).

The advent of the International Argo Progam has provided the oceanographic community with unprecedented, year-round coverage of temperature and salinity in the Labrador Sea. A composite of data from Argo floats in the Labrador Sea is presented in Figure 6. The time series clearly demonstrates the seasonal and interannual variability observed over the last decade in this region. The deep convection event of 2008 is evident in both the temperature and salinity fields. The Argo composite indicates that the winter of 2011 was similar to the preceding winter with very limited convection (mixed layer depths might fluctuate between 200 and 400 m). Deep convection was down to 1400 m in 2012, which is clearly shown by temperature and salinity data from Argo floats. The salinity in the top 200 m in 2012 was the lowest since 2003, particularly in the top 50 m. Convection also occurred in the winter of 2013, but it was not as deep as in the previous year, and mostly limited to the top 1000 m. The situation changed quite significantly in 2014. Wintertime cooling that triggered convective mixing homogenized the top 1600 m or even 1800 m layer of the water column in the central region of the Labrador Sea.

The hydrographic survey of the AR7W line, conducted in May of 2014 (Figure 7), shows that the convective mixing that took place in the previous winter reached 1600 m to 1800 m depth and possibly deeper, which is consistent with the analysis based on Argo profiles (Figure 6). It seems possible that the source of convection was limited in area, but that convection was prolonged in duration so that the newly-mixed water spread from its local source out and across the Labrador Sea. The cold and less saline water mass layer below 3000 m is clearly shown in the hydrographic data from this survey. Due to heavy ice conditions on the Labrador Shelf in 2014, the two most inshore AR7W station could not be sampled.

Other than being the main factor of interannual variability of the intermediate layer throughout the North Atlantic, wintertime convection in the Labrador Sea is a key process in the Atlantic Meridional Overturning Circulation (AMOC), and the Labrador Sea is one of the few areas in the global ocean where surface water is exchanged with the deep ocean. It also has an important role in biogeochemical cycling in the Labrador Sea, and strong convection enhances the entrainment of gases such as oxygen and carbon dioxide into the deep water from the atmosphere, as well as from surface freshwater.

Total Inorganic Carbon and pH

About one quarter of carbon dioxide (CO_2) released by human activities (anthropogenic CO_2, mainly due to fossil fuel combustion) has been taken up by the oceans, altering the basic ocean chemistry, specifically the marine carbonate system. The dissolution of anthropogenic CO_2 has decreased ocean pH by 0.1 units over the past 200 years, corresponding to a 30% increase in acidity (Caldeira and Wickett, 2003). If global emissions of CO_2 continue at their present rate, ocean pH is predicted to fall an additional 0.3 units by 2100. The oceans have not experienced such a rapid pH decrease (ocean acidification) or one of this great a magnitude for at least 20 million years (Feely et al., 2004), raising serious concerns about the ability of marine ecosystems to adapt. The major impact of decreasing pH will be felt by organisms that form calcium carbonate ($CaCO_3$) shells and skeletons, because rising acidity increases the solubility of $CaCO_3$. Since $CaCO_3$ shells and skeletons are naturally more soluble at lower temperatures and higher pressures, high latitude and deep water ecosystems will be more vulnerable to the added stress of ocean acidification. Furthermore, rapid environmental changes such as retreating ice extent and enhanced hydrological cycles may amplify these problems.

Arctic outflow and the local uptake of anthropogenic CO_2 in the deep convection region of the Labrador Sea are major controlling mechanisms of the state of ocean acidification in the Northwest Atlantic. The Arctic water flows to the highly productive regions in the Northwest Atlantic, which have important commercial fisheries, make these regions more susceptible to future ocean acidification than others (Azetsu-Scott et al., 2010). The Labrador Sea is the site of a strong "solubility pump"; anthropogenic CO_2 sequestration from the atmosphere is transported to the deep ocean by chemical and physical processes. In the newly ventilated Labrador Sea water (NV-LSW), which ranges between 150-500m deep for stations in the central part of the Labrador Basin, DIC increased by 15.5 μmol kg^{-1} from 1996 to 2014, due to the local uptake of anthropogenic CO_2 (Figure 8). As a result, the pH decreased by 0.07 units (in the total pH scale) during the same period (Figure 8) representing a decline rate of 0.0032 y^{-1}, higher than the global average of 0.002 y^{-1}. Despite the slight differences observed in the metrics over the last few years, observed trends between 1996 to 2014 remain highly significant with R^2 explaining respectively 85.4% and 79.5% of the variance for DIC and pH. Ocean acidification influences the capacity of the ocean uptake of CO_2 from the atmosphere. Continued monitoring of the chemical state and investigation of biological responses to ocean acidification in the Northwest Atlantic are urgently needed.

Silicate

Nutrient concentrations are important controlling parameters, together with light, for productivity of phytoplankton. For diatoms, silicate often regulates their bloom (Egge and Aksnes, 1992). In Norwegian and Barents Seas, a decrease in silicate concentration in winter was reported in the Atlantic water mass over the past 20 years (Rey, 2012). In the Labrador Sea, a decline in silicate concentration has been observed for the newly ventilated Labrador Sea Water (150-500m), which represents the winter mixed layer (Figure 9). This decrease in silicate was 0.07 μmol/kg/year during the period of 1991 to 2014.

Transient tracers CFC-12 and SF6

During the second half of the twentieth century, the atmospheric burden of chlorofluorocarbons (CFCs) increased steadily due mainly to their widespread use as refrigerants and aerosol propellants. The invasive atmospheric flux of these mostly inert gases provides an excellent record of ocean circulation, and profiles of dissolved CFC-12 concentration have been measured annually along the AR7W line since 1991. As a consequence of restrictions on the manufacture and use of ozone depleting substances introduced in 1989,

the atmospheric mixing ratio of CFC-12 has been in decline since 2003 and so it is becoming less useful as a tracer of very recent ventilation. Measurements of an alternative transient tracer, sulphur hexafluoride (SF6), were introduced in 2011. There has been a rapid near-linear increase in atmospheric SF6 since around 1980 and dissolved concentration profiles show enhanced structure in recently ventilated water compared with CFC-12. Figure 10 shows dissolved concentrations of SF6 and CFC-12 along the AR7W line in May 2014. Figure 11 shows mean concentrations of CFC-12 and SF6 in newly-ventilated Labrador Sea Water (150<500 m depth in Labrador Sea Central Basin) from 1991 to present.

Ocean colour from remote sensing

Ocean colour, as an indicator of sea surface chlorophyll-*a* (SSC), is derived from observations from the Moderate Resolution Imaging Spectroradiometer (MODIS) aboard the Aqua Earth Observing System satellite. Remotely-sensed images of ocean colour for the Labrador Sea are composited on a 2-week basis from the beginning of March to the end of October each year. From November to February, the data are too sparse to be useful. From these composites, ocean colour data are extracted from 511 pixels comprising the AR7W transect. A biweekly climatology of chlorophyll-*a* constructed from the time series of ocean colour from 2003 to 2014 (Figure 12) indicates that the annual spring bloom of phytoplankton starts and ends earlier on the Labrador and Greenland Shelves (mid-April to early June) compared to the central Labrador Basin (early May to late June). However in 2014 timing of the blooms were particularly late only starting at the beginning in the first week of May on the Greenland Shelf and late May on the Labrador Shelf, later than normal by two to three weeks. It is also worth mentioning the observation of strong bloom on the Labrador Shelf in October with concentrations of chlorophyll over 2 mg m^{-3}. Within the two-dimensional spatial regional boxes defined by Harrison and Li (2008), the concentration of sea surface chlorophyll averaged over the period from March 2014 to October 2014, SSC was 0.46 mg m^{-3} on the Labrador Shelf, 0.71 mg m^{-3} in the central Labrador Basin, and 0.59 mg m^{-3} on the Greenland Shelf. The annual average normalized anomalies for 2014 were respectively -0.72, -0.32, and -0.40, the three regions all being below normal (Figure 13).

Phytoplankton

Upper ocean (z<100m) phytoplankton sampled on AR7W in the spring and early summer from 1994 to 2014 shows region-specific characteristics (Figure 14). The Greenland Shelf is a region with high concentrations of chlorophyll-*a* and nanophytoplankton, but low concentrations of picophytoplankton. Conversely, the central Labrador Basin is a region with lower concentrations of chlorophyll-*a* and nanophytoplankton, but high concentrations of picophytoplankton and bacteria. The Labrador Shelf has the lowest concentrations of chlorophyll-*a* and nanophytoplankton, but intermediate concentrations of picophytoplankton. During the most recent sampling period of May 2014, concentrations of chlorophyll-*a* in all 3 regions appeared to be among the lowest regionally-specific values ever recorded (Figure 14). Upper ocean (z<100m) temperatures were also at the low end of the recorded spectrum with the exception of the Greenland Shelf that was around average. For program resource reasons, the time series of picophytoplankton, nanophytoplankton, and bacteria were discontinued in 2013.

Mesozooplankton

One species of copepod, *Calanus finmarchicus*, dominates the mesozooplankton biomass throughout the central region of the Labrador Sea, while on the shelves *C. finmarhicus*, *C. glacialis* and *C. hyperboreus* each contribute aout one third (Head et al. 2003). *C. finmarchicus* abundances show regional variations that are generally consistent from year-to-year and are related to regional differences in the timing of the life-cycle events, which are themselves influenced by environmental conditions. During the winter of 2013-2014 intense and deep convection in the central Labrador Sea seems to have delayed the spring season in 2014 leading to a low abundance of the *Calanus finmarchicus* (Figure 14). On the Labrador Shelf, *C. finmarchicus* abundances are generally relatively low in spring (Figure 14), as it was the case in 2014. In spring, populations here generally have few young stages from the new years' generations, but their abundances increase in summer when they dominate the populations. In spring 2011, however, there were many more young stages than usual: the reason for this is not clear. There was no significant trend in springtime abundance of *C. finmarchicus* between 1996 and 2014 on the Labrador Shelf. In the Central Labrador Sea,

total *C. finmarchicus* abundance is generally relatively low in spring and summer, with a low proportion of young stages; one exception being the summer of 1995, when young stages were dominant and total abundance was relatively high. There was no trend in springtime total abundance between 1996 and 2014 in the Central Labrador Sea and the abundance in 2014 was near the lower values seen in previous springs. *C. finmarchicus* abundances are generally higher in the eastern Labrador Sea than farther west in spring, because the spring bloom starts earlier here, which leads to earlier reproduction in *C. finmarchicus*. Abundances are generally higher here in summer than in spring, with the highest concentration of all occurring in spring 2006. The abundance in 2014 was at the low end of the range of values seen in previous springs, and there was no trend in springtime abundance between 1996 and 2014. PDI% represents the proportion of Copepodite C1 to C3 over the entire population express in percent and shows the proportion of recently produced younger stages within each region. In all three regions the PDIs were among the lowest observed between 1995 and 2014 (Figure 14).

Calanus glacialis and *Calanus hyperboreus*, which are both Arctic species, are more abundant in the Arctic waters covering the shelves than in the central basin (Head et al. 2003). The abundance of *C. glacialis* and *C. hyprboreus* in spring 2014 were below average in all three regions except for *C. hyperboreus* on the Greenland shelf. Low abundance may be partly explained by the unavailability of a fraction of the population still in diapause below 100m, due to the delayed arrival of the spring season (Figure 15).

In 2014, abundances of euphausiids as well were generally below average on the Labrador and the Greenland shelf and slope, but remained relatively unchanged over the last few years in the central basin. Gastropoda abundance is mainly represented by larval stages hard shelled "snail like" organisms, which are found at intermediate depths in the water column and are most likely among the first that will be directly impacted by the lowering of the pH. Their abundance in 2014 was lower than average on the Labrador Shelf, where they are certainly more abundant than within the 2 other regions (Figure 15).

Continuous Plankton Recorder (CPR)

The Continuous Plankton Recorder (CPR) is an instrument that is towed by commercial ships that collects plankton at a depth of ~7 m on a long continuous ribbon of silk (~260 µm mesh). The position on the silk corresponds to location of the different sampling stations. CPR data are analysed to detect differences in the indices of phytoplankton (colour and relative numerical abundance) and zooplankton relative abundance for different months, years or decades in the northwest Atlantic. The indices indicate relative changes in concentration (Richardson et al. 2006). The sampling methods from the first surveys in the northwest Atlantic (1960 for the continental shelf) to the present are exactly the same so that valid comparisons can be made between years and decades.

The tow routes between Reykjavik and the Gulf of Maine are divided into eight regions: the Western Scotian Shelf (WSS), the Eastern Scotian Shelf (ESS), the South Newfoundland Shelf (SNL), the Newfoundland Shelf (NS) and four regions in the NW Atlantic sub-polar gyre, divided into 5 degree of longitude bins (Figure 16). In this report a broad-scale comparison is presented for CPR data collected in all regions and all sampling decades. More detailed analyses for the Scotian Shelf and Newfoundland Shelf regions are presented in the AZMP Reports from the Maritimes and Newfoundland Regions. These latter reports concentrate on results from data collected since 1992, since these are comparable to AZMP survey results, which date back to 1999.

Monthly abundances (log10(N+1) transformed for all but PCI[1]) were calculated for 15 CPR taxa by averaging values for all individual samples collected within each region for each month and year sampled. Monthly averages for each region and year were then averaged over each decade prior to 2009, (i.e. for 1960-1969, 1970-1979, 1980-1989, 1990-1999 and 2000-2009) to give decadal annual average abundances. Monthly averages were similarly averaged for 2010-2012 to give a tri-annual average abundance, and for 2013 to give an annual average abundance. For the shelf regions and in the 25-30˚W region there was insufficient sampling during the 1980s to calculate decadal annual abundances. January and December were never sampled during the 1980s for the three regions between 30˚W and 45˚W: these missing values were calculated as the averages of the monthly values for the 1970s and 1990s. Linear interpolation was used to fill in values for the missing months in 2013, when there were 2 or 3 missing months for the WSS and ESS,

[1] PCI – Phytoplankton colour index, a semi-quantitative measure of total phytoplankton abundance.

respectively and 1 in all other regions, except the SNL where there was sampling in only 7 months so that no annual abundance could be calculated. Decadal (1960s, 1970s, 1980s, 1990s, 2000s), tri-annual (2010-2011) and annual (2013) standardized abundance anomalies were calculated for each region based on the climatological averages and standard deviations calculated using the decadal annual averages between the 1960s and 2000s.

Phytoplankton

The phytoplankton colour index (PCI).

The climatological annual averages (1960-2009) for the phytoplankton colour index (PCI) are highest in the two Newfoundland Shelf regions (NS, SNL), intermediate in the Scotian Shelf (WSS, ESS) and lower in the regions between 25 and 45˚W (Figure 17). Decadal average PCI values increased in all regions between the 1970s and 1990s and remained high thereafter in the sub-polar gyre, but decreased in shelf regions in the 2000s and 2010-2012. In 2013 PCI annual average anomalies were very high in the sub-polar gyre and on WSS and close to those of the 1990s and 2000s for the NS and ESS.

Diatoms

The climatological annual abundance for diatoms is highest in the NS, lower in the other shelf regions and lowest in the sub-polar gyre. Decadal annual abundances increased after the 1970s, with highest values in the 1990s (ESS) or 2000s (other regions). In 2010-2012 abundance anomalies remained high in the sub-polar gyre and decreased in shelf regions, while in 2013 they increased still further in the sub-polar gyre, and decreased slightly in shelf regions (Figure 17).

Dinoflagellates

The climatological annual abundance for dinoflagellates is highest on the SNL shelf, intermediate in the other shelf regions and lower in the sub-polar gyre. Dinoflagellate abundance increased after the 1970s with highest values in the 1990s (ESS, WSS) or 2000s (other regions). In 2010-2012 dinoflagellate abundances were similar to those of the 2000s, except in the two regions east of 35˚W, where they declined. In 2013, abundance anomalies increased on the WSS, remained high in the NS and 40-50˚W regions, and decreased or remained low elsewhere (Figure 17).

Zooplankton

Calanus I-IV

The climatological annual average abundance for *Calanus* I-IV (mostly *Calanus finmarchicus*) is similar in all regions except the NS, where it is higher (Figure 18). In the sub-polar gyre decadal abundances have generally increased over the decades, with the highest abundance anomalies in 2010-2012. In 2013 there was a substantial decrease in *Calanus* I-IV abundance in the 40-45ºW region, and slight decreases in the other three sub-polar gyre regions. For shelf regions decadal annual abundances have generally decreased over the decades, with little change in the NS and SNL regions after 2010. By contrast, on the WSS and ESS there were dramatic decreases in *Calanus* I-IV abundance in 2010-2012, which were followed by equally dramatic increases in 2013.

Calanus finmarchicus V-VI

The climatological annual average abundance for *C. finmarchicus V-VI* is slightly higher on the NS than elsewhere, and slightly lower on the SNL (Figure 19). In the sub-polar gyre decadal annual abundances have generally increased, and these increases have persisted through 2010-2012 and 2013, except in the 40-45°W region where, as for *Calanus I-IV*, there was a decrease in 2013. For shelf regions decadal annual abundance anomalies were higher in the 1970s than in other decades, except on the NS, where the 1960s had the highest value. There were marked decreases in *C. finmarchicus V-VI* abundance in 2010-2012 on the NS, WSS and ESS. In 2013 these decreases were reversed, especially on the WSS, which had an unusually high abundance.

.

Calanus glacialis V-VI

The climatological annual average abundance for *C. glacialis* is higher on the NS than in the other regions. Decadal abundance anomalies increased in all regions over the decades with maximum values in the 2000s or in 2010-2012. In 2013 *C. glacialis* abundance decreased everywhere relative to 2010-2012 and the 2000s.

Calanus hyperboreus III-VI

The climatological annual average abundance for *C. hyperboreus* is higher on the NS than elsewhere. In most regions decadal abundance anomalies increased from relatively low values in the 1960s and 1970s to higher values in 1990s or 2000s. In 2010-2012 abundances in the sub-polar gyre were high in the two western regions and low in the two eastern regions, and high on the WSS. In 2013 abundances were relatively low everywhere, except the WSS.

Small copepod taxa (Copepod nauplii, Paracalanus/Pseudocalanus, Oithona spp.)

Three small copepod groups have higher climatological annual average abundances in shelf regions (NS and to the west) than in the sub-polar gyre (Figure 19). In the sub-polar gyre decadal annual abundances of copepod nauplii and *Paracalanus/Pseudocalanus* increased over the decades, with highest levels in the 2000s. Thereafter they either decreased slightly in 2010-2012, increasing again in 2013 (copepod nauplii) or remained high in 2010-2012, decreasing in 2013 (*Paracalanus/Pseudocalanus*). For shelf regions the decadal annual abundances of copepod nauplii increased between the 1970s and 1990s and remained high (NS) or decreased (SNL, ESS, WSS) in the 2000s and thereafter, with an especially low value on the ESS in 2013. Abundance anomalies for *Paracalanus/Pseudocalanus* showed inconsistent changes over the decades in shelf regions, although there were low values in all 4 regions in the 2000s, followed by an increase (NS) or decrease (WSS, ESS) in 2010-2012, and a decrease (NS) or increase (WSS, ESS) in 2013. Changes in decadal annual abundances for *Oithona* spp. were inconsistent over the decades, although abundances were generally relatively high in the 1960s or 2000s in the sub-polar gyre and in the 1990s in shelf regions. In 2010-2012 abundances in the 40-45˚W and 35-40˚W regions were unusually high, and in 2013, while the level in the 35-40˚W region dropped dramatically, all other regions except the ESS had high *Oithona* spp. abundances.

Macrozooplankton

The climatological annual average abundances of euphausiids and hyperiid amphipods are both mainly higher in the deep ocean regions of the sub-polar gyre and highest in the 40-45˚W region (Figure 20). Euphausiid abundance was generally highest in the sub-polar gyre in the 1990s and in shelf regions in the 1970s, and was low everywhere in 2010-2012. In 2013 levels remained low everywhere except on the NS and ESS. Abundances of hyperiid amphipods have generally increased everywhere over the decades, and were high in 2010-2012 and 2013, except in the 25-30˚W region and on the ESS.

Acid-sensitive taxa

Coccolithphores, phytoplankton that are covered with calcite scales, and foraminifera (forams) whose shell composition includes calcium carbonate, have been counted in CPR samples only since 1992. They are generally more abundant in the sub-polar gyre than on the shelves, although coccolithophores are also abundant on the SNL (Figure 21). Coccolithophore and foram abundances were higher in 2010-2012 than in the 1990s or 2000s and these high values persisted in 2013, except for dramatic decreases in the levels of both on the ESS, and slight decreases in the 35-40˚W region. Pteropods of the genus *Limacina* have shells that are composed of aragonite, which is a form of calcium carbonate that is especially sensitive to dissolution at low pH. The climatological annual abundance of *Limacina* shows a more-or-less flat distribution across all regions. Over the decades there has been a general upward trend in abundance for *Limacina* in regions east of the Scotian Shelf, while abundances there have fluctuated. In 2010-2012 abundances were generally relatively high in all regions, except for the ESS and the 30-35˚W regions. In 2013 *Limacina* abundance decreased in the sub-polar gyre, while levels remained high in shelf regions.

Continuous Plankton Recorder (CPR) – Summary & Discussion

In terms of the climatological (1960-2009) annual average abundances, six of the 15 CPR taxa analysed for this report are generally more abundant in shelf regions than the sub-polar gyre: the three phytoplankton

taxa and the three "small copepod" taxa. All three phytoplankton taxa were more abundant everywhere in the 1990s and/or 2000s than in previous decades although since 2010 there have been increases or decreases in abundance, varying by region and taxon. Changes in abundance of the small copepod taxa have been mainly positive over the decades in the deep ocean, with abundances generally peaking in the 1990s in shelf regions.

The boreal *Calanus* species *C. finmarchicus* (which includes the categories *Calanus* I-IV and *C. finmarchicius* V-VI) has been increasing in abundance in the sub-polar gyre in recent years, while abundances in shelf regions have varied considerably. The Arctic *Calanus* species, *C. glacialis* and *C. hyperboreus*, are more than 10 times less abundant than *C. finmarchicus*, and changes in abundance in the different regions are likely linked to changes in Arctic inflow.

Euphausiids and hyperiids both show high climatological annual average abundances in regions between 25 and 45˚W, where waters of both Atlantic and Arctic origin occur. Euphausiids are more associated with Atlantic water and hyperiids more with Arctic water, so that the generally increasing trend in abundance for the former and decreasing trend for the latter suggest an increased contribution of Arctic water in recent decades.

The changes in pH that have resulted from increasing carbon dioxide levels in the atmosphere have not yet been great enough to elicit negative effects on any of the three acid-sensitive taxa. All three taxa were relatively abundant in 2010-2012, but in 2013 coccolitophore and foram abundances decreased markedly on the ESS, and Limacina levels decreased throughout the sub-polar gyre. These changes may be linked to changes in stratification for the coccolithophores (Raitsos et al. 2006) and food supply and/or contribution of Arctic water for the other two.

Summary

The Labrador Sea is a key component of the global ocean circulation system and provides one of the few sites where deep convection during the winter serves to exchange surface waters with the deep ocean and, in the process, entrain gases such as carbon dioxide and oxygen. Fisheries and Oceans Canada has carried out long-term environmental monitoring of the Labrador Sea through the Atlantic Zone Off-Shelf Monitoring Program (AZOMP; http://www.bio.gc.ca/science/monitoring-monitorage/azomp-pmzao/azomp-pmzao-eng.php). This program provides high-quality observations of core variables in a timely manner to the Canadian data archives as well as a number of international data centres (e.g., NODC, ICES, CCHDO, CDIAC). The results presented in this report are summarized in two tables of anomalies for the modelled and remote sensed variables covering seasonally or year round period (Figure 22) and for the variable sampled during the annual survey of the AR7W line (Figure 23).

The NCEP reanalysis of the surface air temperature indicates above normal conditions with an anomaly ranging between 1 – 3°C in the Labrador Sea during the winter for 2013-2014, ~ -1°C below normal for most of Labrador Sea during spring, ~ 1°C above normal for summer, and 0 – 2°C during fall. Sea surface temperature (SST) anomalies in the Labrador Sea mostly followed the patterns observed in air temperature except for the winter when there was mixed SST anomaly pattern, negative and positive in different areas of the Labrador Sea. During the other seasons, positive anomalies were the dominant feature as they were in the air temperature. The Labrador Shelf ice concentration was generally above normal in the winter months of 2014 (reference period: 1979-2000). In the northern part of the Labrador Sea, however, the sea ice concentration was ~25% below normal in January, and interestingly, the same region had ~25% above the normal ice concentration in March. Oceanic heat lost in winter, as shown by the ERA-Interim net heat flux anomaly over the northwest Atlantic, led to winter convection that reached 1800 m in 2014, significantly deeper than the 1000 m seen in the previous year. The deepest part of the intermediate layer, the 1800-2500 m layer, in the central Labrador Sea has been gradually warming since the mid-1990s. The variations in hydrographic characteristics of the upper layer across the Labrador Sea have been recently documented and described by Yashayaev et al. (2015). Local ocean cooling and heating are not the only factors determining these characteristics, and other factors are considered in this work; this will be further studied and documented by AZOMP with particular emphasis given to Arctic and Greenland discharges of freshwater.

About one quarter of carbon dioxide (CO_2) released by human activities (anthropogenic CO_2, mainly by fossil fuel combustion) has been taken up by the oceans, altering the basic ocean chemistry, specifically the marine carbonate system, thus leading to a decrease ocean pH by 0.1 units over the past 200 years. Total inorganic carbon (TIC) and pH have been monitored over the period 1996-2014 in the newly ventilated water masses (150–500 m) of the central part of the Labrador Basin. Both DIC and pH have shown regular opposite trends, indicating an uptake of anthropogenic CO_2 that translates in a continuous lowering of pH. DIC increased by 15.5 µmol kg^{-1} from 1996 to 2014, due to the local uptake of anthropogenic CO_2. As a result, pH has decreased by 0.07 units (in the total pH scale) during the same period at a rate of 0.0032 units y^{-1}. This is higher than the global average of 0.002 y^{-1}. Silica in the Labrador Sea exhibits the same decreasing trend as the rest of the North Atlantic with a decrease of 0.07µmol kg^{-1} y^{-1} between 1991 and today.

The extreme atmospheric and physical ocean events in the winter of 2014 had profound impacts on the biological properties of the Labrador Sea that were evident until at least the middle of the summer. According to MODIS satellite imagery, the spring bloom initiation was particularly late in the Labrador Sea, only starting at the beginning of May on the Greenland Shelf and late May on the Labrador Shelf, later than normal by at least three weeks. This resulted in below normal annual average normalized chlorophyll-*a* anomalies for 2014 for the Labrador Shelf, central basin and the Greenland Shelf of -0.72, -0.32, and -0.40, respectively. These effects were reflected by the mesozooplankton communities: *Calanus finmarchicus* abundance in 2014 being among the lowest values observed since monitoring started in 1994. The Population Development Index (PDI), which shows the proportion of recently produced young stages within a region, corroborates the observed lag in the spring bloom. In all three regions the observed indices were among the lowest observed between 1995 and 2014.

Acknowledgements

We would like to thank Blair Greenan for his helpful comments and suggestions. The NCEP Reanalysis data were provided by the NOAA-CIRES Climate Diagnostics Center, Boulder, Colorado, USA. The sea ice concentration anomaly data are the US National Snow and Ice Data Center. The authors wish to thank the many staff and associates at BIO have contributed to the AZOMP which was carried out by the Ocean and Ecosystem Sciences Division in 2014. These efforts, together with those of the officers and crew of CCGS Hudson, are gratefully acknowledged.

References

Azetsu-Scott, K., A. Clarke, K. Falkner, J. Hamilton, E. P. Jones, C. Lee, B. Petrie, S. Prinsenberg, M. Starr and P. Yeats (2010), Calcium Carbonate Saturation States in the waters of the Canadian Arctic Archipelago and the Labrador Sea, 115, C11021, doi:10.1029/2009JC005917 Journal of Geophysical Research.

Barnston, A. G., and R. E. Livezey (1987), Classification, seasonality and persistence of low-frequency atmospheric circulation patterns. Mon. Wea. Rev., 115, 1083-1126.

Caldeira, K., and M. E. Wickett (2003), Anthropogenic carbon and ocean pH, Nature, 425, 365

Climate Prediction Center (2010), NOAA/National Weather Service, National Centers for Environmental Prediction. Camp Springs, MA. http://www.cpc.noaa.gov/products/precip/CWlink/daily_ao_index/ao.shtml#publication

Egge, J., and Aksnes, D.L. (1992), Silicate as regulating nutrient in phytoplankton competition. Mar. Ecol. Prog. Ser. **83**(2-3): 281–289. doi: 10.3354/meps083281.

Fetterer, F., K. Knowles, W. Meier, and M. Savoie (2002), updated 2011. Sea ice index. Boulder, CO: National Snow and Ice Data Center. Digital media.

Feely, R. A., C. L. Sabine, K. Lee, W. Berelson, J. Kleypas, V. J. Fabry,and F. J. Millero (2004), Impact of anthropogenic CO_2 on the $CaCO_3$system in the oceans, Science, 305, 362–366.

Harrison, W.G. and W.K.W. Li (2008), Phytoplankton growth and regulation in the Labrador Sea: light and nutrient limitation. J. Northwest. Atl. Fish. 39:71-82.

Hauser, T., Demirov, E., Zhu, J. and I Yashayaev (2015), North Atlantic atmospheric and ocean inter-annual variability over the past fifty years – Dominant patterns and decadal shifts. Progress in Oceanography, Volume 132, March 2015, Pages 197–219

Head, E.J.H., Harris, L.R and I Yashayaev. (2003), Distributions of *Calanus* spp. and other mesozooplankton in the Labrador Sea in relation to hydrography in spring and early summer (1995-2000). Prog. Oceanogr. 59: 1-30

Hurrell, J. W. (1995), Decadal trends in the North Atlantic Oscillation: Regional temperatures and precipitation. Science, 269, 676-679.

Josey, S., J. Grist, D. Kieke, I. Yashayaev, and L. Yu (2015), Sidebar: Extraordinary ocean cooling and new dense water formation in the North Atlantic [in "State of the Climate 2014"], Bull. Amer. Meteor. Soc.

Kalnay, E., M. Kanamitsu, R. Kistler, W. Collins, D. Deaven, L. Gandin, M. Iredell, S. Saha, G. White, J. Woollen, Y. Zhu, M. Chelliah, W. Ebisuzaki, W. Higgins, J. Janowiak, K.C. Mo, C. Ropelewski, J. Wang, A. Leetmaa, R. Reynolds, R. Jenne, and D. Joseph (1996), The NCEP/NCAR 40-Year Reanalysis Project., Bull. Amer. Meteor. Soc., 77, No. 3, 437-470.

Raitsos, D.E., Lavender, S.J., Pradhan, Y., Tyrrell, T., Reid, P.C., Edwards, M. (2006), Coccolithophore bloom size variation in response to the regional environment of the subarctic North Atlantic. Limnol. Oceanogr. 51: 2122-2130.

Rey, F. (2012), Declining silicate concentrations in the Norwegian and Barents Seas. ICES J. Mar. Sci. J. Cons. **69**(2): 208–212

Richardson, A.J., Walne, John, A.W.G., Jonas, T.D., Lindley, J.A., Sims, D.W., Stevens, D. and M. Witt,(2006), Using continuous plankton recorder data. Prog. Oceanogr. 68: 27-74.

Visbeck, M.H., J.W. Hurrell, L. Polvani and H.M. Cullen (2001), The North Atlantic Oscillation: Past, Present and Future. Proc. Nat. Acad. Sci., 98, 12876-12877 doi: 10.1073/pnas.231391598

Yashayaev, I. (2007), Hydrographic changes in the Labrador Sea, 1960-2005, Progress in Oceanography, 73, 242-276.

Yashayaev, I., and J.W.Loder (2009), Enhanced production of Labrador Sea Water in 2008. Geophys. Res. Lett., 36: L01606, doi:10.1029/2008GL036162.

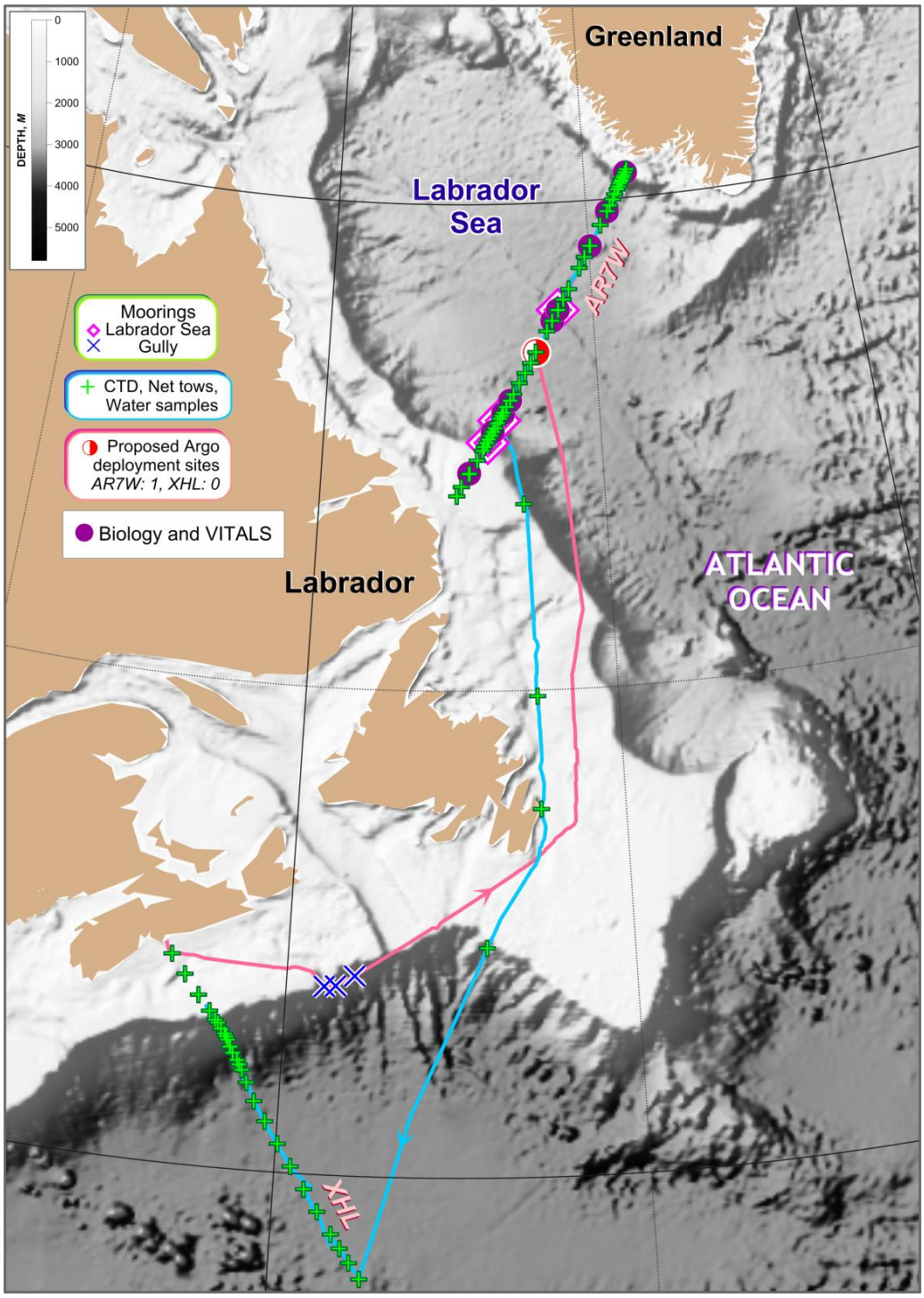

Figure 1: Schematic of the Labrador Sea component of the DFO Atlantic Zone Offshore Monitoring Program (AZOMP). Standard stations along the sections are shown as green plus signs, mooring sites are indicate by purple open lozenge and blue cross (AMAR listening device), and circles indicate the location of biology and VITALS casts. Location of Argo profiler deployments are indicated by the red/white circles.

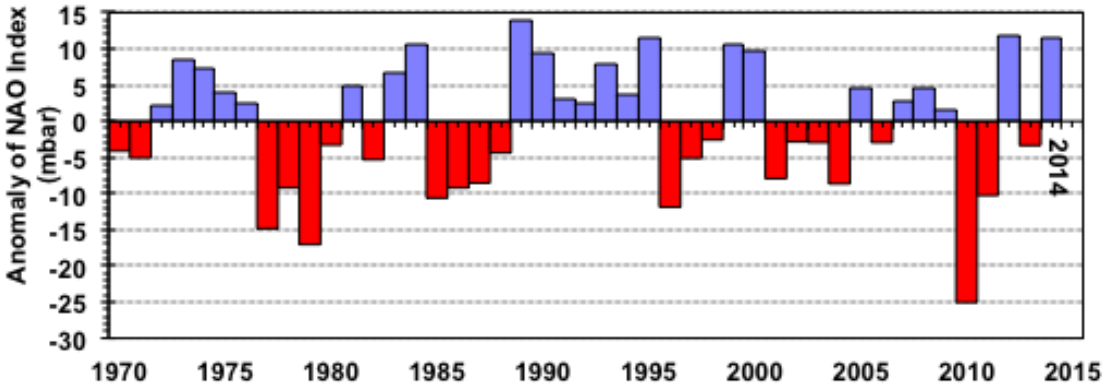

Figure 2: Average Sea Level Pressure for Dec, Jan, Feb in mbar (Winter North Atlantic Oscillation Index)

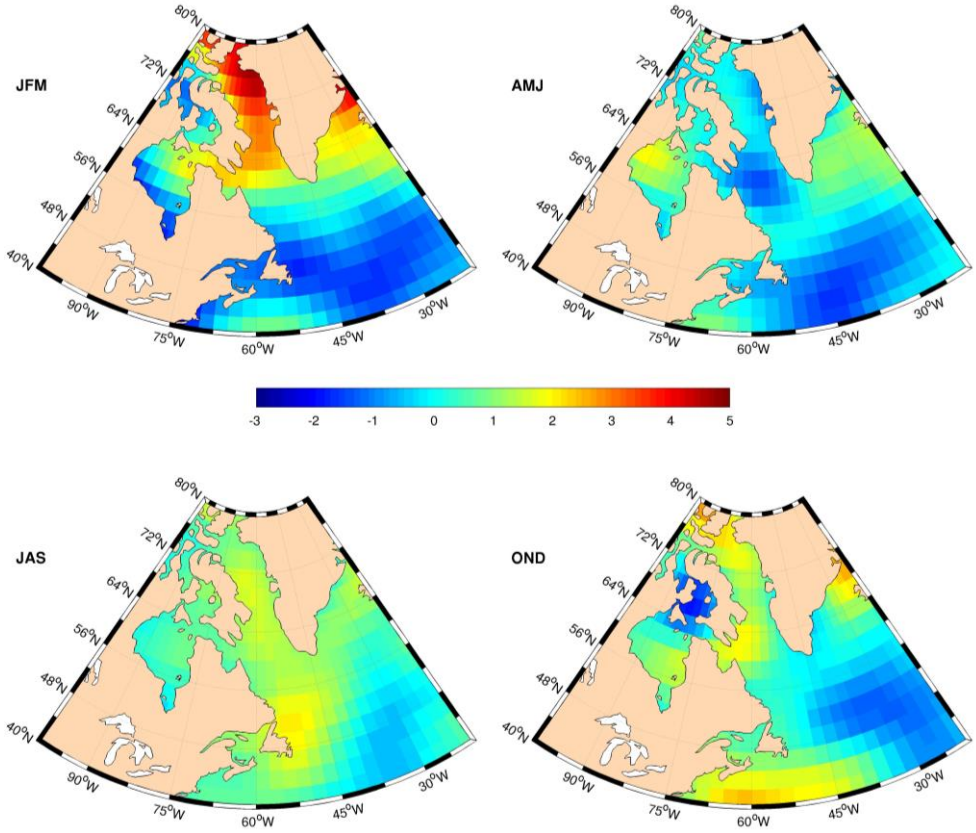

Figure 3: Surface air temperature anomaly for winter, spring, summer and fall periods in 2014 as derived from NCEP/NCAR reanalysis. http://www.esrl.noaa.gov/psd/

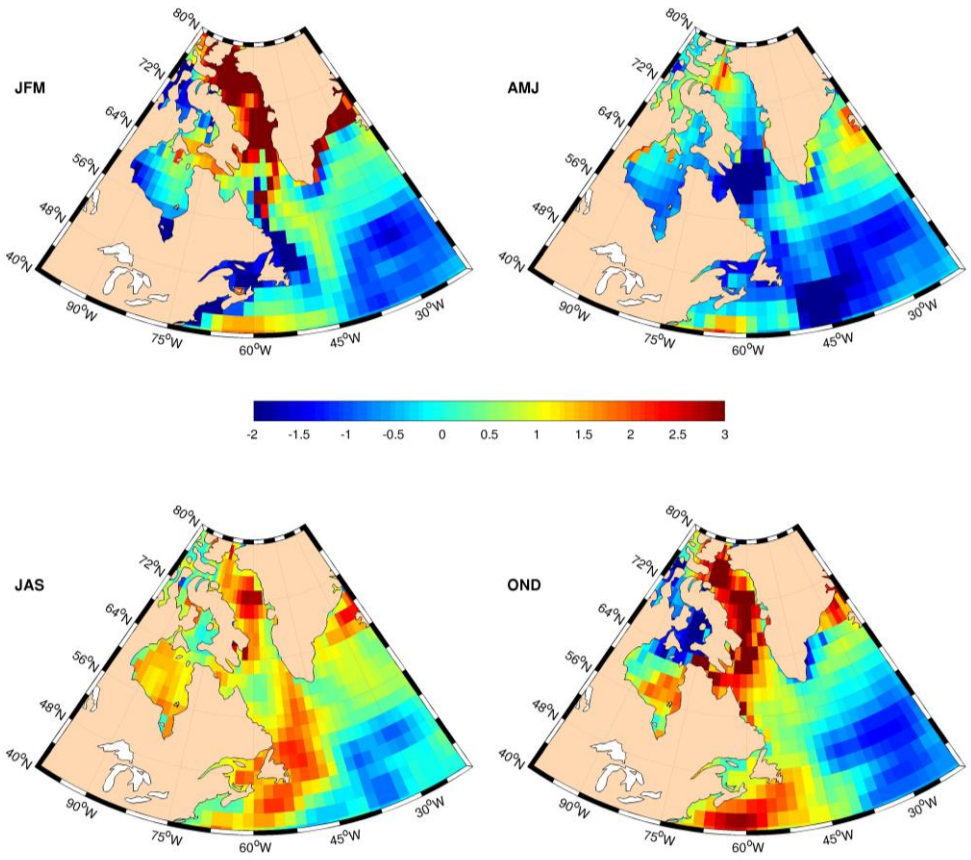

Figure 4: Sea surface temperature anomalies for winter, spring, summer and fall 2014 derived from NCEP/NCAR reanalysis. http://www.esrl.noaa.gov/psd/

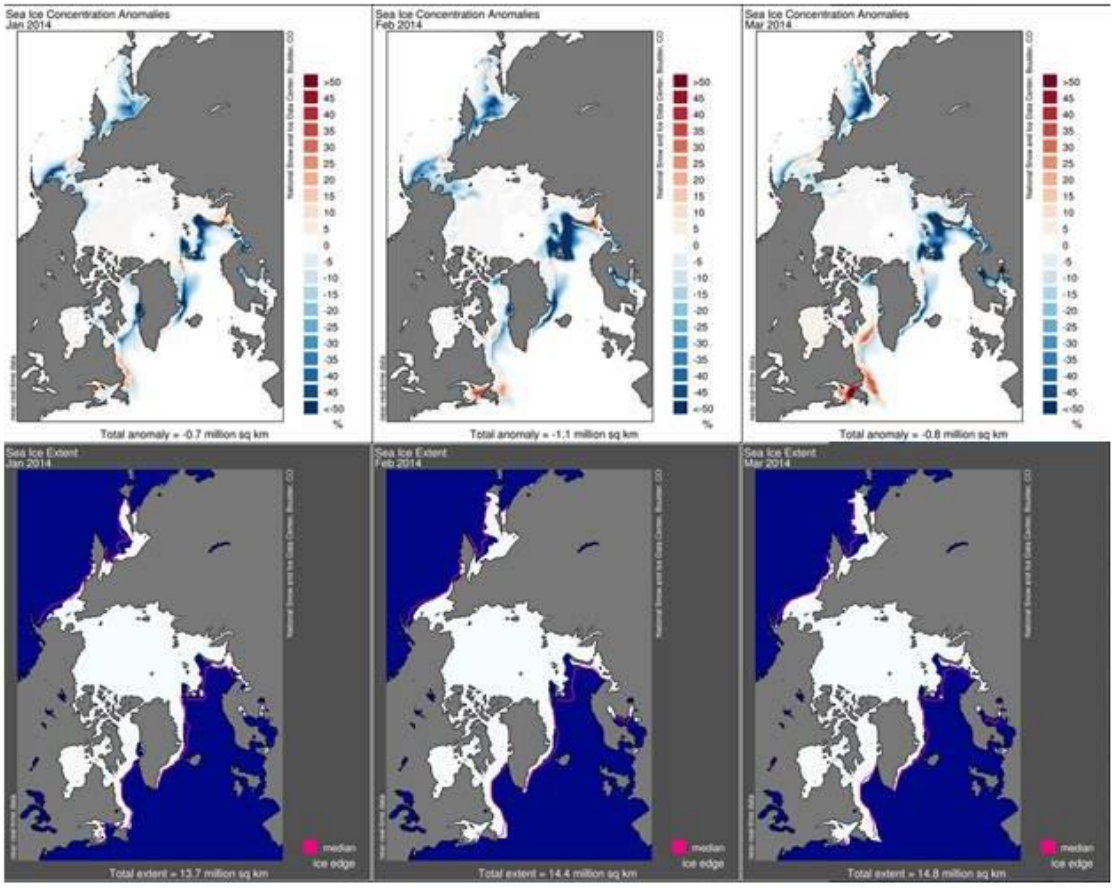

Figure 5. Sea ice concentration anomalies (A) and sea ice extent (B) for Jan-Mar 2014 as derived by the US National Snow and Ice Data Center (reference period 1979-2000) http://nsidc.org/data/seaice_index/archives/index.html

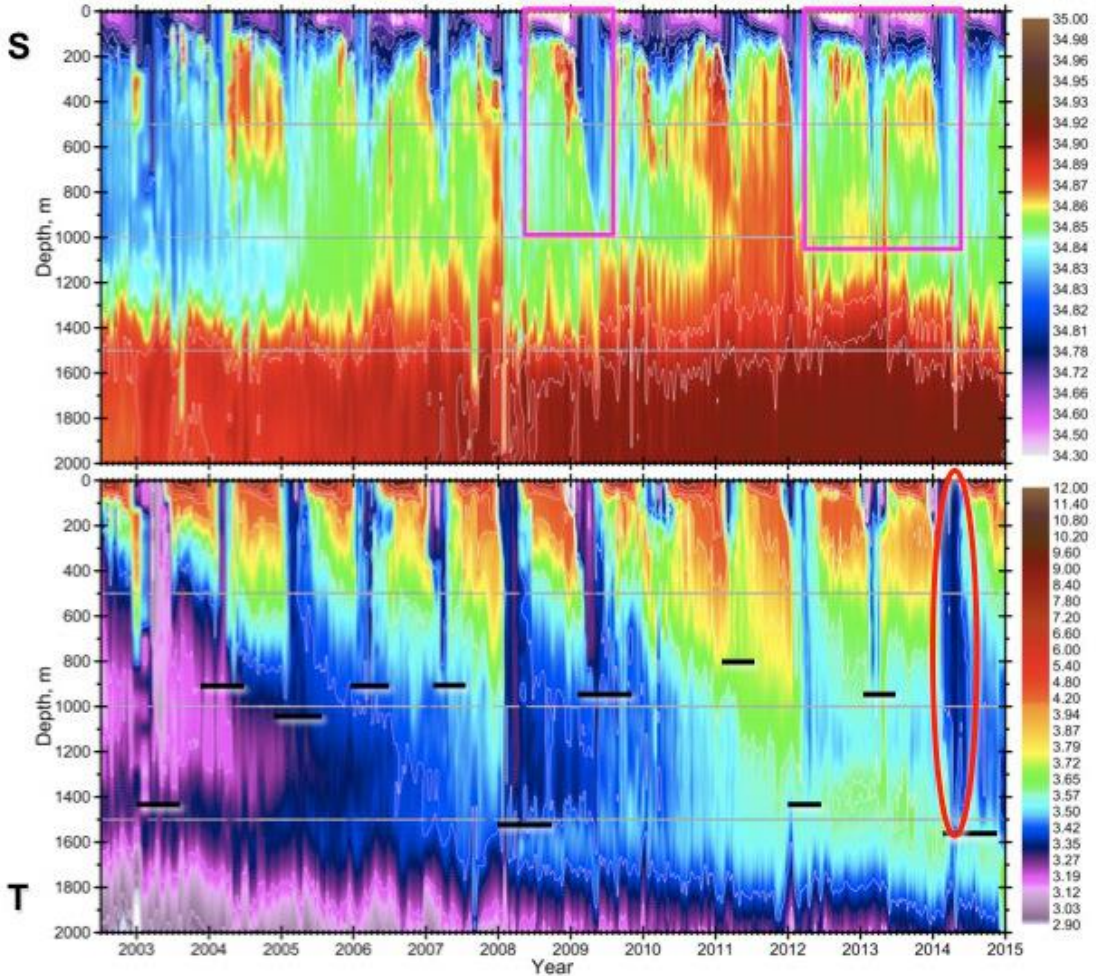

Figure 6: Salinity (top) and potential temperature (bottom) from Argo drifters in the Labrador Sea. The winter deep convection event of 2008, 2012 and 2014 have clearly extend beyond 1400m. Convection was limited to a depth of about 200 m in the winters of 2010 and 2011

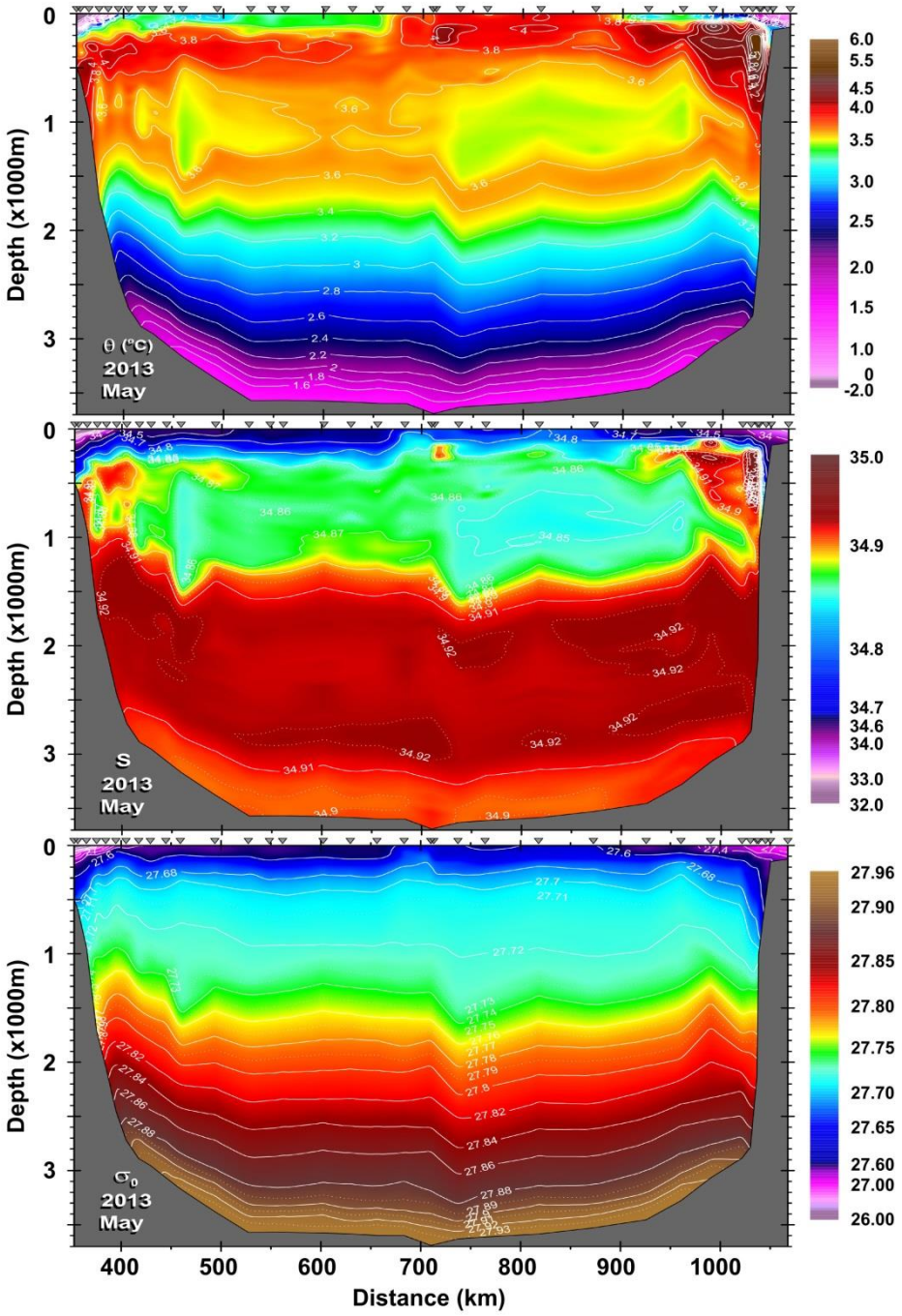

Figure 7: Labrador Sea (AR7W Section) potential temperature (top), salinity (middle) and potential density (bottom).

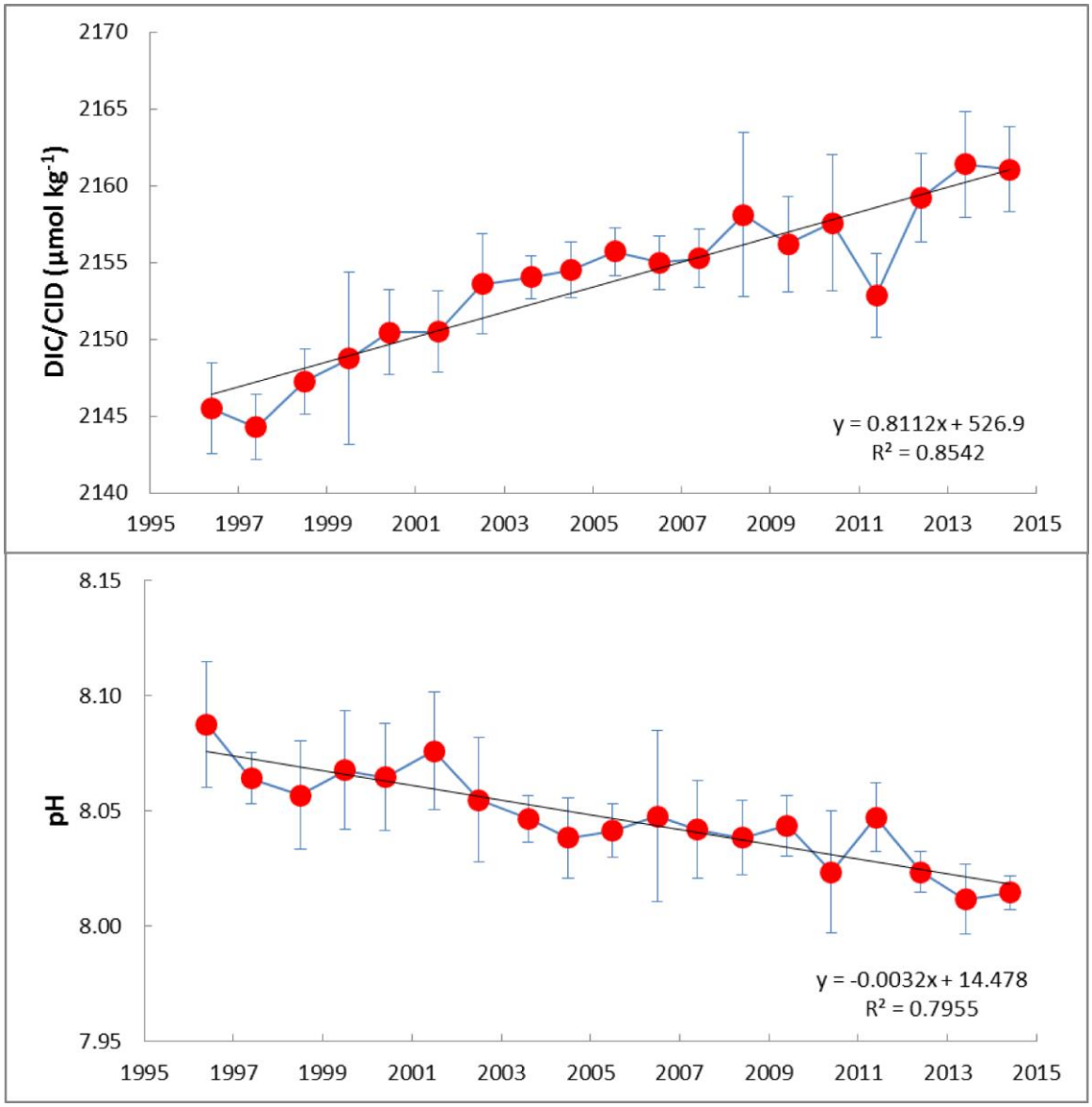

Figure 8: Time series of total inorganic carbon (TIC) and PH, top panel for TIC, bottom panel from PH. TIC and PH in in the 150–500 m depth range and corresponding regression lines for stations in the central part of the Labrador Basin for the period 1996–2014

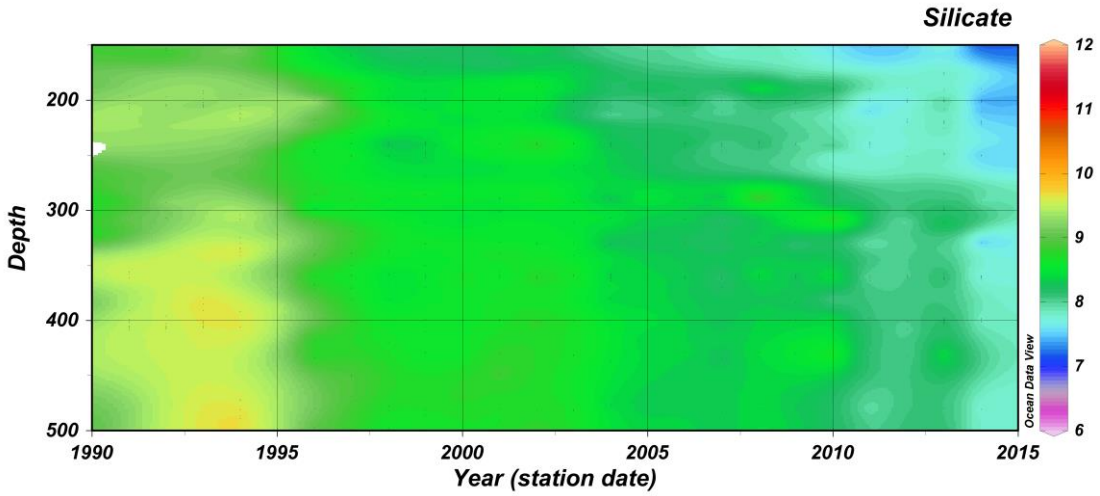

Figure 9: Silicate concentration (µmol/kg/year) observes within the newly ventilated Labrador Sea Water (150-500m) in May 2014 on the AR7W line.

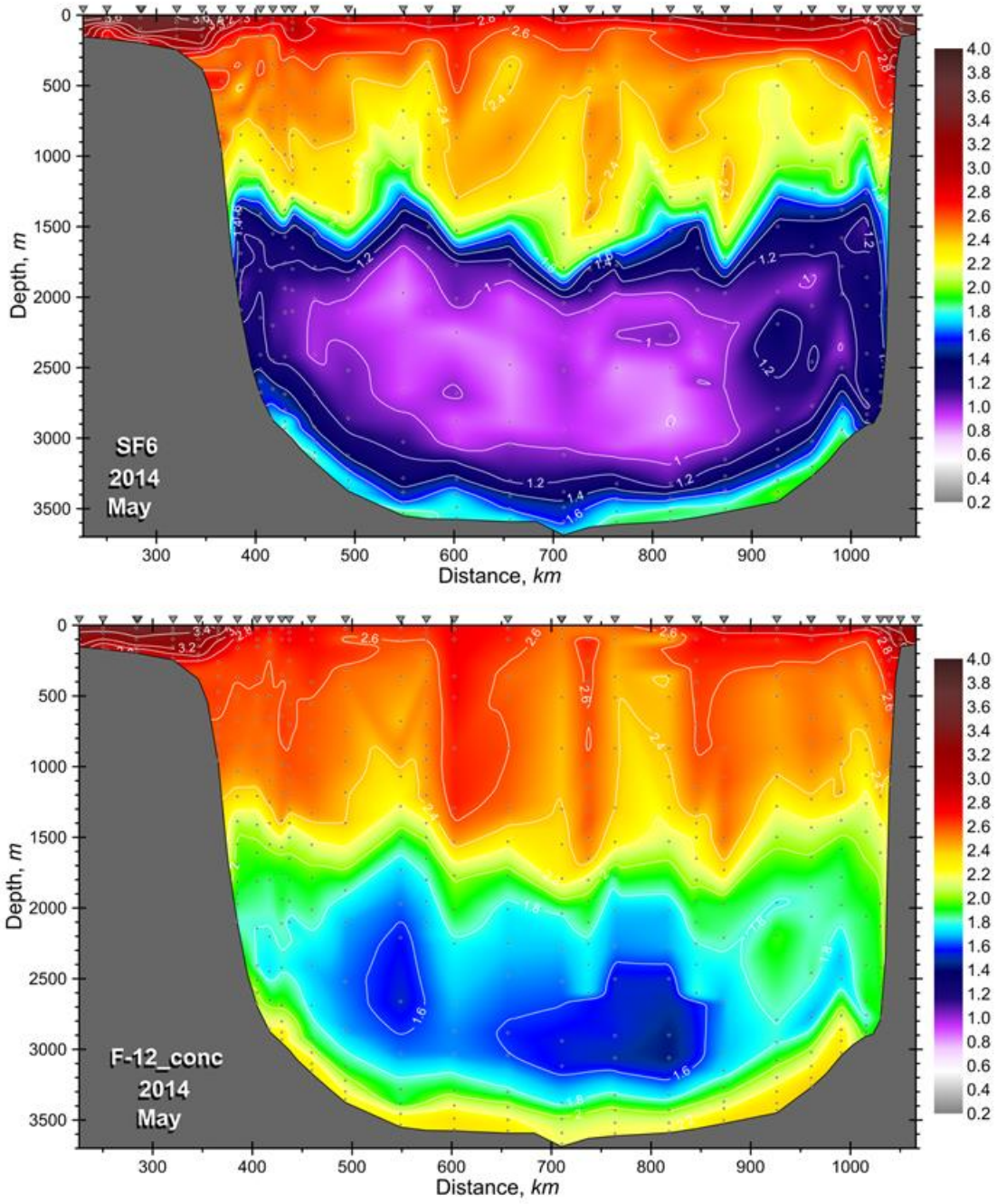

Figure 10: Profiles of transient tracers along the AR7W section. Top: dissolved SF_6 concentration in units of 10^{-15}moles per kilogram seawater. Bottom: CFC-12 concentration in units of 10^{-12} moles per kilogram.

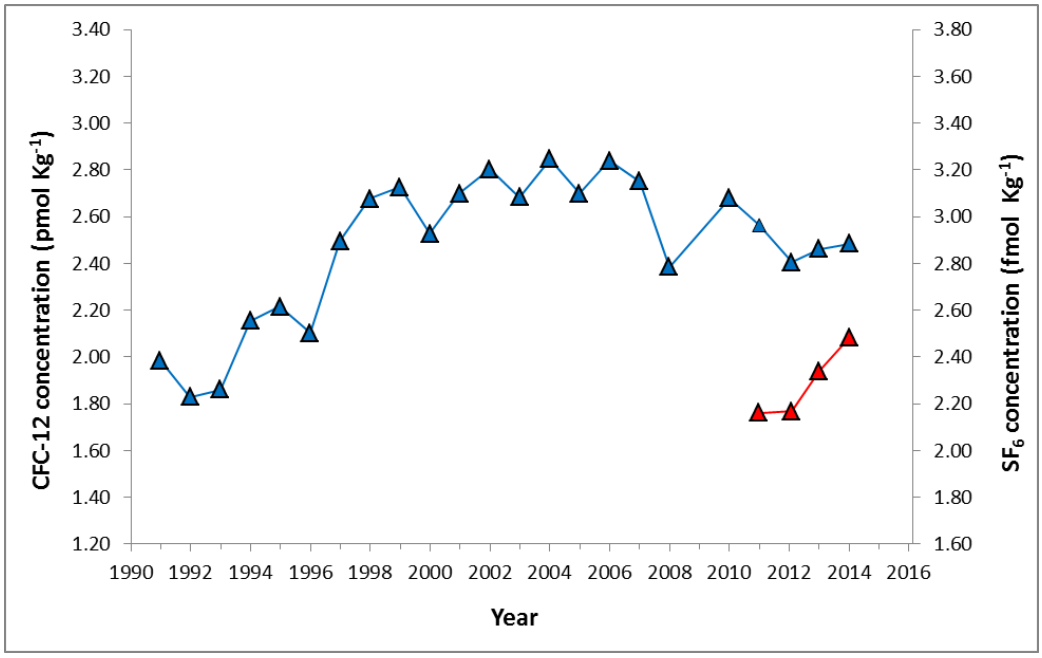

Figure 11**:** Annual mean concentrations of CFC-12 (blue) and SF_6 (red) in newly-ventilated Labrador Sea Water (defined as 150<500 m in the central part of the Labrador Sea Basin) from 1991 to present. SF_6 measurements began in 2011.

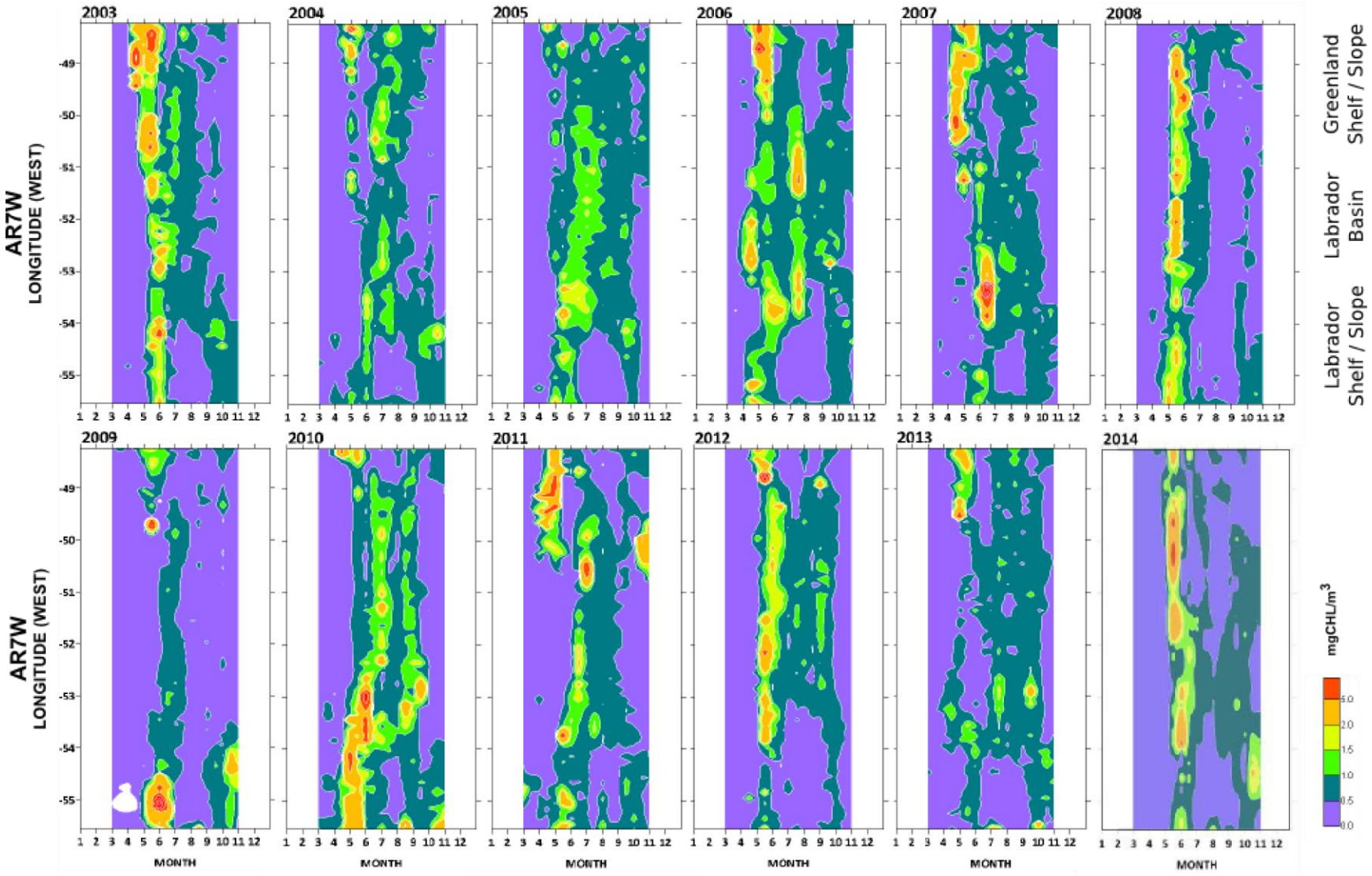

Figure 12: The concentration of sea surface chlorophyll-*a* estimated from remotely-sensed ocean colour at 2-week intervals from March to October spanning a 10-year time series, 2003-2014.

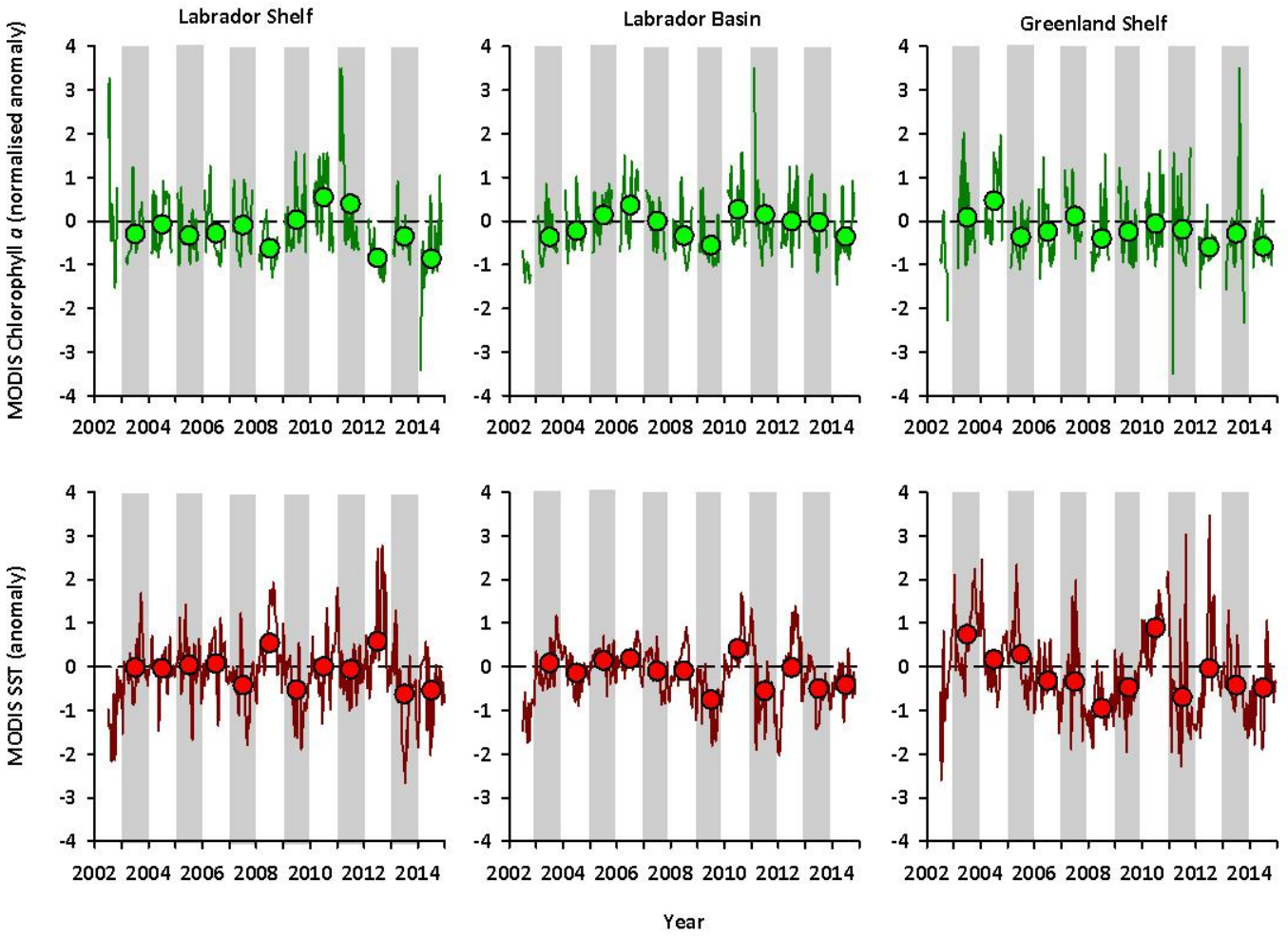

Figure 13: Chlorophyll-*a* normalized anomaly and SST anomaly time series (2003-2014) for Labrador shelf (left column), Labrador Basin (middle column) and Greenland Shelf (right column) estimated from bi-weekly MODIS data. Lines indicate biweekly anomalies, circles indicate annual average anomalies.

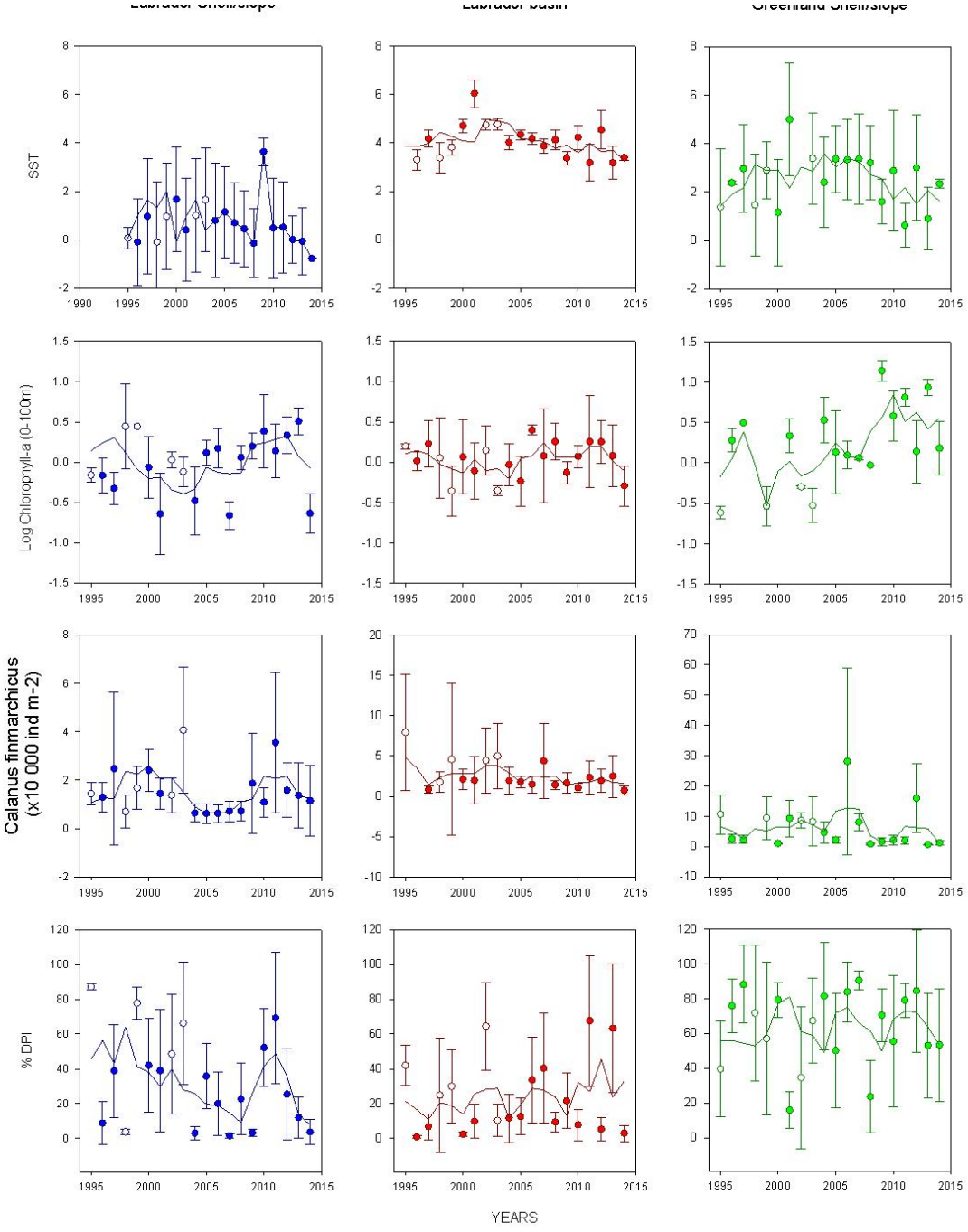

Figure 14: Upper ocean (z<100m) average SST and concentrations of phytoplankton, *Calanaus finmarchicus* abundance and %PDI (from top to bottom panel) on AR7W sampled in spring or early summer from 1994 to 2014. Circles indicate mean value for stations designated within each region, error bars indicate among-station standard deviation, and heavy line indicates 3-year running average of the time series.

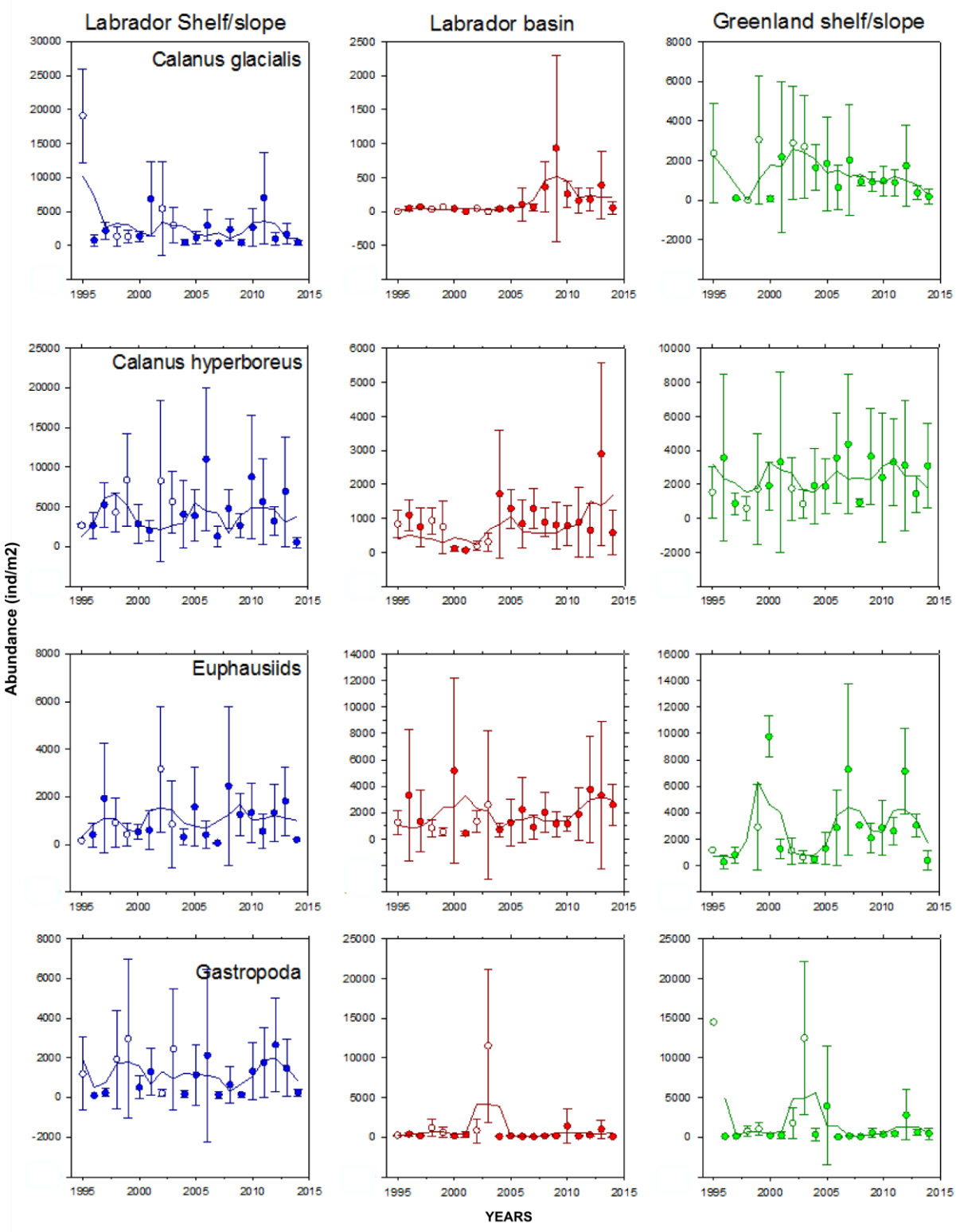

Figure 15: Time series of *C. glacialis*, *C. hyperboreus*, Euphausids and Gastropoda and from Spring – Summer 1995 - 2014. Full circles show results for years when sampling was in spring; open circles show results for years when sampling was in summer.

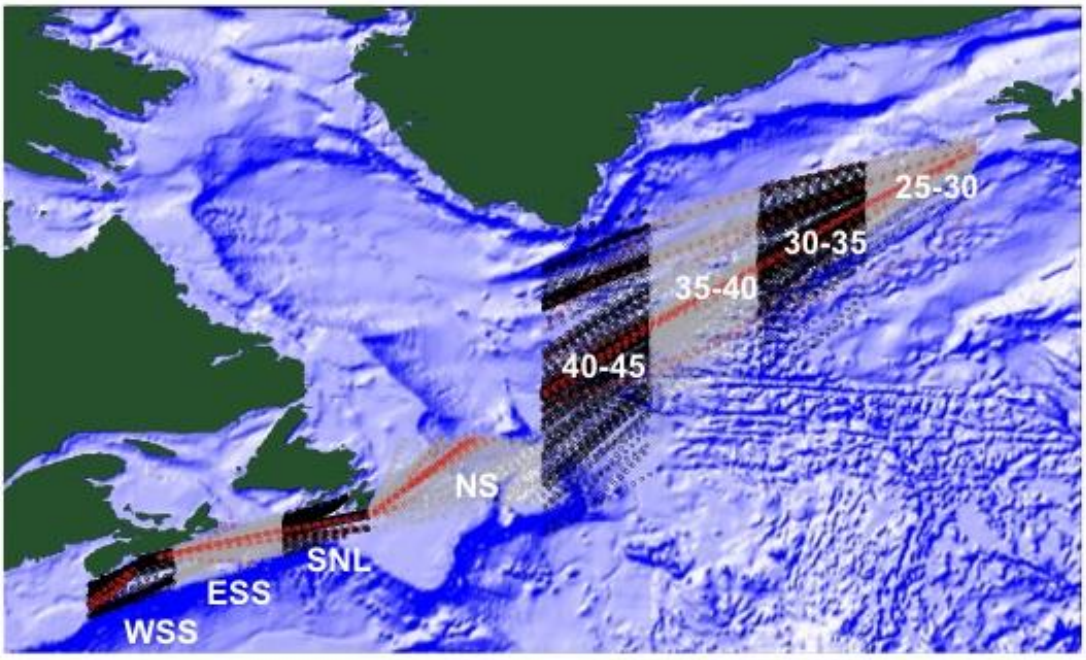

Figure 16: Continuous Plankton recorder (CPR) lines and stations 1957 to 2013. Stations sampled in 2013 are shown in red. Data are analysed by region. Regions are: Western Scotian Shelf (WSS), Eastern Scotian Shelf (ESS), South Newfoundland Shelf (SNL), Newfoundland Shelf (NS), and between longitudes 40-45°W, 35-40°W, 30-35°W, 25-30°W.

.

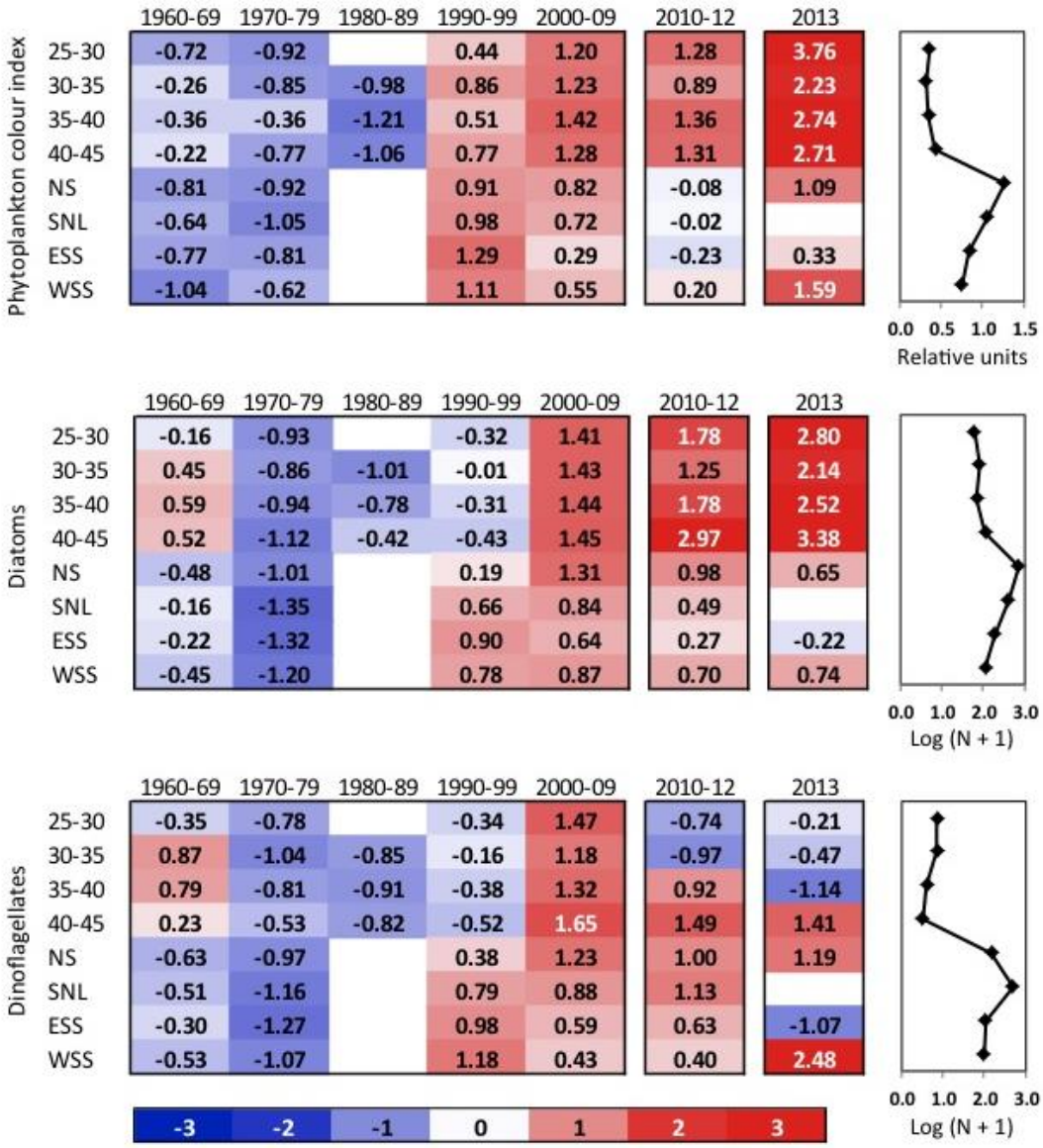

Figure 17: CPR time series for the annual averages for three indices of phytoplankton concentration, calculated from monthly averages over decadal (1960-2009), tri-annual (2010-2012) or annual (2013) periods for eight regions in the NW Atlantic. Blank cells correspond to years or decades where sampling was too sparse to give annual values. Red (blue) cells indicate higher (lower) than normal values. The climatological averages were calculated from the decadal annual averages between 1960 and 2009, and are shown in the panels on the right. The numbers in the cells are the standardised anomalies. The regions are: Western Scotian Shelf (WSS), Eastern Scotian Shelf (ESS), South Newfoundland Shelf (SNL), Newfoundland Shelf (NS), and between longitudes 40-45°W, 35-40°W, 30-35°W, 25-30°W.

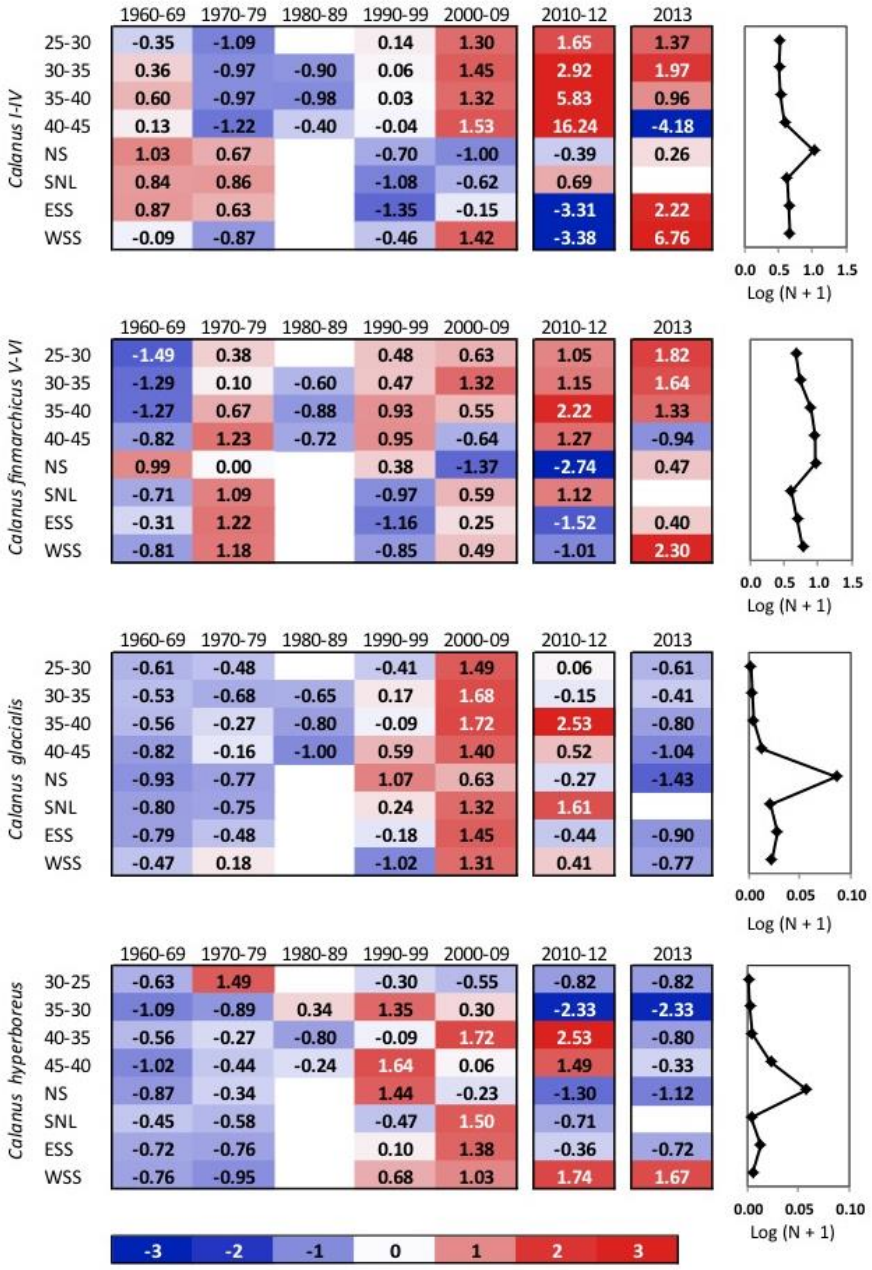

Figure 18: CPR time series for the annual average abundances for four Calanus taxa, calculated from monthly averages over decadal (1960-2009), tri-annual (2010-2012) or annual (2013) periods for eight regions in the NW Atlantic. Blank cells correspond to years or decades where sampling was too sparse to give annual values. Red (blue) cells indicate higher (lower) than normal values. The climatological averages were calculated from the decadal annual averages between 1960 and 2009, and are shown in the panels on the right. The numbers in the cells are the standardised anomalies. The regions are: Western Scotian Shelf (WSS), Eastern Scotian Shelf (ESS), South Newfoundland Shelf (SNL), Newfoundland Shelf (NS), and between longitudes 40-45°W, 35-40°W, 30-35°W, 25-30°W.

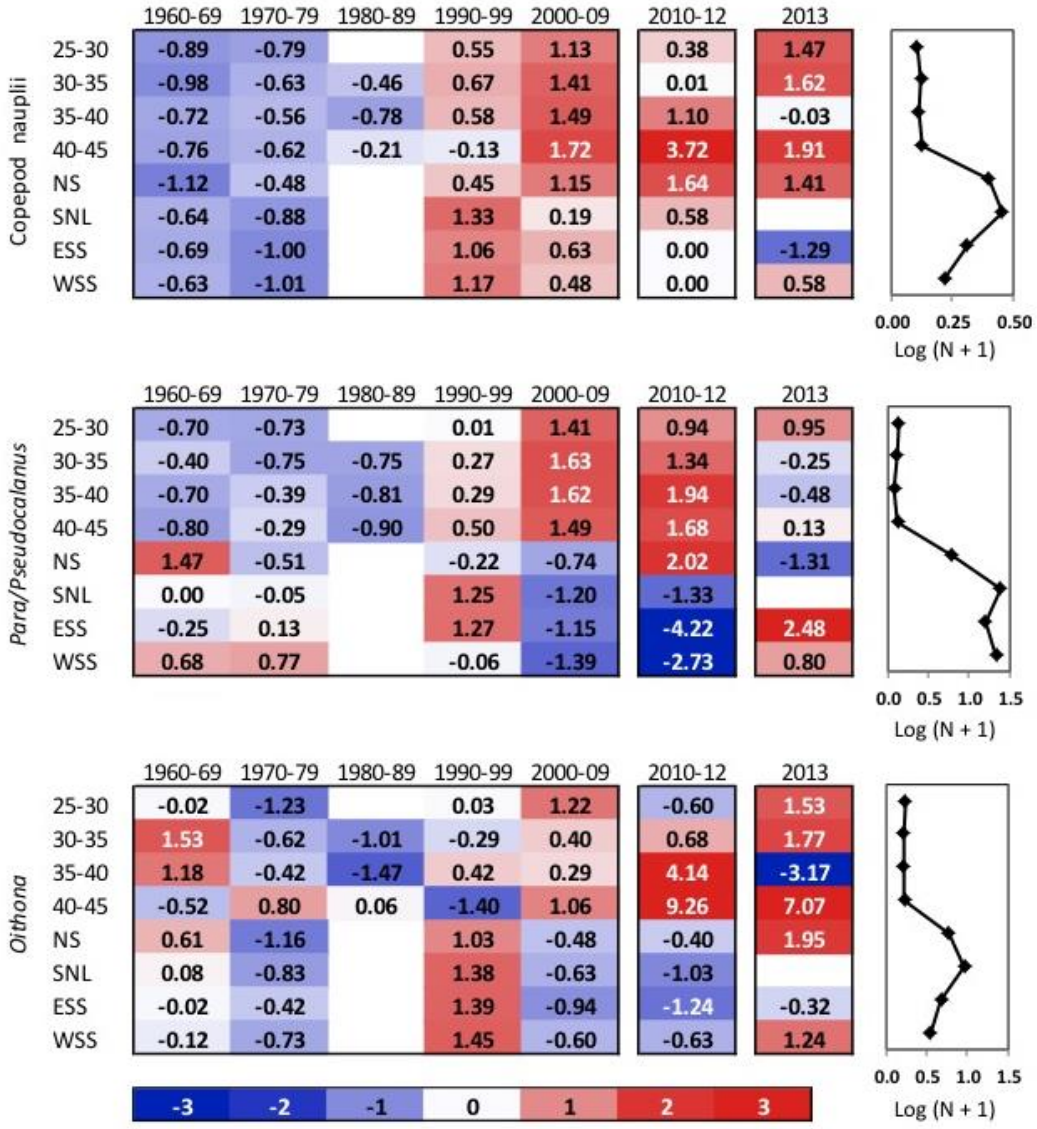

Figure 19: CPR time series for the annual average abundances for three small copepod taxa, calculated from monthly averages over decadal (1960-2009), tri-annual (2010-2012) or annual (2013) periods for eight regions in the NW Atlantic. Blank cells correspond to years or decades where sampling was too sparse to give annual values. Red (blue) cells indicate higher (lower) than normal values. The climatological averages were calculated from the decadal annual averages between 1960 and 2009, and are shown in the panels on the right. The numbers in the cells are the standardised anomalies. The regions are: Western Scotian Shelf (WSS), Eastern Scotian Shelf (ESS), South Newfoundland Shelf (SNL), Newfoundland Shelf (NS), and between longitudes 40-45°W, 35-40°W, 30-35°W, 25-30°W.

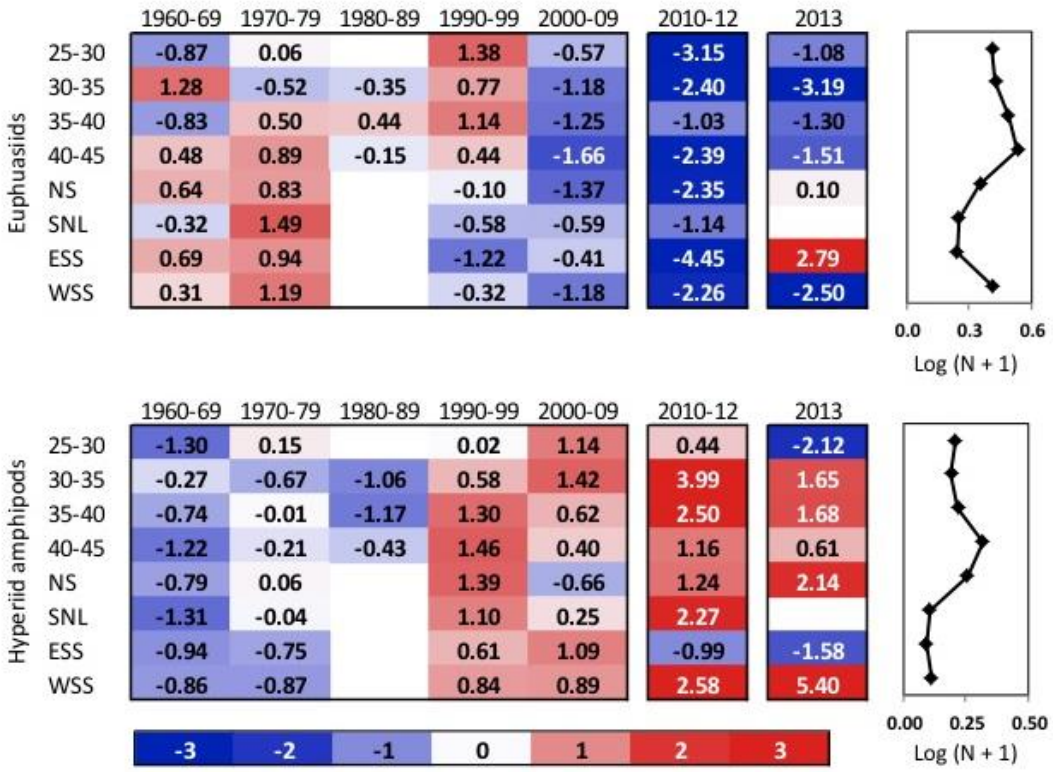

Figure 20: CPR time series for the annual average abundances for two macrozooplankton taxa, calculated from monthly averages over decadal (1960-2009), tri-annual (2010-2012) or annual (2013) periods for eight regions in the NW Atlantic. Blank cells correspond to years or decades where sampling was too sparse to give annual values. Red (blue) cells indicate higher (lower) than normal values. The climatological averages were calculated from the decadal annual averages between 1960 and 2009, and are shown in the panels on the right. The numbers in the cells are the standardised anomalies. The regions are: Western Scotian Shelf (WSS), Eastern Scotian Shelf (ESS), South Newfoundland Shelf (SNL), Newfoundland Shelf (NS), and between longitudes 40-45°W, 35-40°W, 30-35°W, 25-30°W.

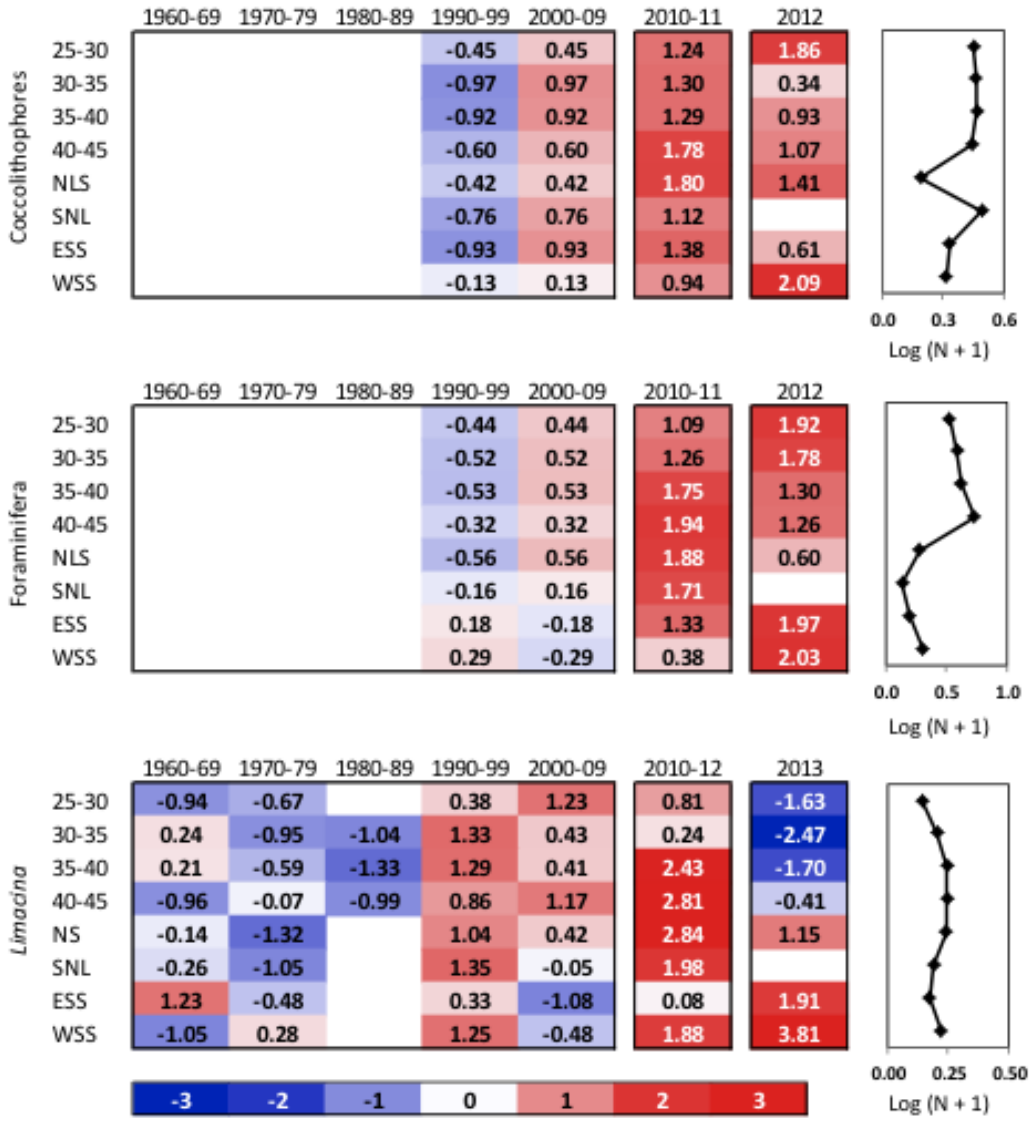

Figure 21: CPR time series for the annual average abundances for three acid-sensitive taxa, calculated from monthly averages over decadal (1960-2009), tri-annual (2010-2012) or annual (2013) periods for eight regions in the NW Atlantic. Blank cells correspond to years or decades where sampling was too sparse to give annual values. Red (blue) cells indicate higher (lower) than normal values. The climatological averages were calculated from the decadal annual averages between 1990 and 2009 for the coccolithophores and foraminifera, and between 1960 and 2009 for Limacina, and are shown in the panels on the right. The numbers in the cells are the standardised anomalies. The regions are: Western Scotian Shelf (WSS), Eastern Scotian Shelf (ESS), South Newfoundland Shelf (SNL), Newfoundland Shelf (NS), and between longitudes 40-45°W, 35-40°W, 30-35°W, 25-30°W.

	Year																				
	1994	1995	1996	1997	1998	1999	2000	2001	2002	2003	2004	2005	2006	2007	2008	2009	2010	2011	2012	2013	2014
Winter NAO*	0.53	1.38	-1.16	-0.42	-0.15	1.29	1.21	-0.73	-0.18	-0.19	-0.81	0.62	-0.19	0.45	0.64	0.29	-2.60	-0.98	1.42	-0.23	1.39
Air Temperature - Winter	-1.67	-0.96	1.02	-1.02	0.36	1.43	-0.21	1.18	0.27	1.12	3.51	1.60	3.44	3.03	-1.94	2.29	4.61	2.60	0.12	2.41	-0.36
- Spring	-0.69	0.78	0.87	1.12	0.65	0.95	-0.06	0.36	0.04	0.01	0.83	2.01	2.10	0.19	1.12	-0.18	2.11	-1.22	1.03	-0.18	-0.28
SST - Winter	-0.84	-0.11	0.19	0.23	0.85	0.88	0.12	0.62	0.77	1.15	2.25	1.34	1.10	1.60	-0.30	1.05	1.84	2.43	0.04	1.55	0.15
- Spring	-0.31	-0.10	0.37	0.75	0.64	0.10	0.06	0.74	-0.19	0.64	0.37	1.00	0.81	0.56	0.20	-0.10	1.49	-0.39	0.29	0.62	-0.29
Ocean colour (Chlorophyll-*a*)																					
Labrador Shelf/Slope									0.33	-0.23	-0.02	-0.27	-0.20	-0.05	-0.50	0.05	0.57	0.43	-0.78	-0.21	-0.81
Central Labrador Sea									-1.12	-0.29	-0.13	0.21	0.34	0.07	-0.29	-0.52	0.27	0.32	0.12	0.10	-0.24
Greenland Shelf/Slope									-0.87	0.14	0.49	-0.33	-0.18	0.18	-0.32	-0.24	-0.04	-0.02	-0.50	-0.27	-0.53
SST anomaly																					
Labrador Shelf/Slope									-1.09	-0.02	-0.05	0.03	0.07	-0.43	0.54	-0.53	0.00	-0.06	0.58	-0.63	-0.54
Central Labrador Sea									-1.04	0.08	-0.14	0.14	0.18	-0.11	-0.10	-0.76	0.41	-0.55	-0.02	-0.50	-0.42
Greenland Shelf/Slope									-0.50	0.74	0.16	0.27	-0.32	-0.35	-0.95	-0.48	0.89	-0.70	-0.05	-0.43	-0.59
Continuous plankton recorder																					
Phytoplankton Colour Index (Based on the climatological values for 1994-2012)																					
WSS	-0.45	2.03	1.01	-1.31	-0.31	2.03	-0.43	0.69	-0.45	-0.05	-0.65	-0.25	-0.29			-0.73	-0.93	-0.72	-0.15	0.80	
EES	-0.73	1.51	1.83	0.27	1.51	-0.17	-1.08	-0.38	0.00	0.20	-0.07	-0.53	-1.09				-1.27	-0.71	-1.56	-0.58	
SNL	-1.38	0.94	0.64	-1.47	1.95	-0.14	-0.68	-0.13		1.09	-0.07	0.2	0.12				-1.16	-0.09	-1.84		
NLS	-0.58	-0.09	2.55	0.31	0.14	-1.52	0.34	0.4	1.21	-0.03	-0.62	-0.39	-0.86				-0.87	-1.58	-1.34	0.44	
40_45	1.19	-0.65	-0.19	-1.97	-0.72	1.68	-0.18	-0.01		0.41	-1.52	0.22	0.2			0.96	-0.6		0.45	2.30	
35_40	0.18	-1.66	0.74		-2.11	0.82	0.05	0.94	0.21	0.12	-1.04	0.44	1.02				0.53		-0.13	1.53	
30_35	0.81	1.58	-0.91		-1.31	0.30	-0.60	0.66	-0.65	0.90	0.47	-0.26	1.04			-1.95	-0.08		-0.76	1.24	
25_30	-0.67	0.32	-1.83		0.25	1.08	-0.72	-0.17		2.25	-0.65	-0.67	0.41			-0.03	0.43		-0.45	1.49	

-3 -2 -1 0 1 2 3

* Inversely scored using a scale from blue to red on the highest to the lowest value

Figure 22. Normalised annual and/or seasonal anomaly of physical and biological variables integrated over large spatial scales estimated using NCEP , remote sensed data or Continuous plankton recorder (CPR) between 1994 and 2013.

Year

	1994	1995	1996	1997	1998	1999	2000	2001	2002	2003	2004	2005	2006	2007	2008	2009	2010	2011	2012	2013	2014
Temperature (0-100m)																					
Labrador Shelf/Slope		-0.99	-1.16	-0.04	0.00	0.68	0.70	-0.64	0.35	1.06	-0.22	0.15	-0.32	-0.58	-1.21	2.78	-0.56	-0.52	-1.06	-1.13	-1.89
Labrador basin		0.23	-1.24	-0.59	0.80	0.83	-1.36	-0.07	0.74	2.72	-0.30	0.18	-0.06	-0.52	-0.13	-1.25	0.01	-1.53	0.49	-1.55	-1.23
Greenland Shelf/Slope		-1.32	-1.24	0.18	-2.67	0.66	-0.33	0.24	-1.53	2.24	-0.31	0.63	0.60	0.64	0.48	-1.10	0.16	-2.05	0.28	-1.79	-0.37
TIC anomalies			-1.59	-1.86	-1.18	-0.84	-0.45	-0.45	0.26	0.36	0.47	0.74	0.58	0.64	1.29	0.86	1.17	0.10	1.54	2.04	1.96
pH anomalies			2.07	0.67	0.23	0.88	0.70	1.38	0.12	-0.37	-0.87	-0.69	-0.31	-0.65	-0.86	-0.55	-1.76	-0.34	-1.75	-2.46	-2.28
Silicate	2.329	1.252	0.839	0.522	-0.356	0.306	0.582	0.177	0.515	-0.162	-0.771	-1.118	-0.168	-1.4	0.011	-1.133	-1.426	-1.653	-1.292	-0.451	-1.445
Chlorophyll-a (Log mg m^3)																					
Labrador Shelf/Slope		-0.16	0.44	0.44	0.03	-0.12	-0.16	-0.32	-0.06	-0.64	-0.48	0.12	0.17	-0.66	0.06	0.20	0.38	0.14	0.33	0.51	-0.63
Labrador bassin	-0.07	0.20	0.01	0.23	0.05	-0.36	0.06	-0.11	0.15	-0.35	-0.03	-0.24	0.40	0.08	0.25	-0.13	0.07	0.26	0.25	0.08	-0.29
Greenland Shelf/Slope	-0.10	-0.62	0.28	0.50		-0.54		0.34	-0.30	-0.53	0.53	0.13	0.10	0.06	-0.03	1.14	0.58	0.81	0.14	0.94	0.18
Mezozooplankton (normalized anomalies)																					
Copepods																					
Labrador shelf/slope		0.85	-0.95	-0.11	0.28	1.65	-0.40	0.21	0.08	1.23	-1.20	-0.58	1.43	-1.87	-0.16	-1.05	0.61	-2.09	-2.39	1.70	-1.51
Labrador bassin		2.82	-0.78	-0.72	-0.05	0.28	-0.57	-0.49	0.71	1.82	-0.68	-0.41	-0.18	-0.26	-0.42	-0.63	-0.44	-1.15	-1.16	-0.52	-0.87
Greenland shel/slope		0.69	-0.84	-0.79	-1.33	0.75	-0.99	0.48	0.59	0.48	-0.52	-0.53	2.77	0.01	-0.97	-0.45	-0.69	-1.31	-1.26	-0.81	-0.68
Calanus finmarchicus																					
Labrador Shelf/Slope		-0.01	-0.81	0.25	-0.08	2.83	-0.17	1.10	1.04	0.00	-0.87	-0.89	-0.89	-0.79	-0.79	0.46	-0.39	2.27	0.15	-0.09	-0.32
Labrador bassin		2.67	-0.54	-0.99	-0.50	0.94	-0.33	-0.40	0.87	1.16	-0.42	-0.50	-0.66	0.83	-0.69	-0.57	-0.88	-0.21	-0.42	-0.14	-1.03
Greenland Shelf/Slope		0.57	-0.59	-0.63	-0.96	0.40	-0.82	0.38	0.29	0.23	-0.29	-0.65	3.10	0.21	-0.84	-0.73	-0.65	-0.67	1.34	-0.86	-0.79
Calanus glacialis																					
Labrador Shelf/Slope		3.43	-0.45	-0.46	0.44	-0.09	-0.58	-0.27	0.20	0.75	-0.64	-0.49	-0.10	-0.67	-0.23	-0.65	-0.16	0.79	-0.52	-0.18	-0.65
Labrador bassin		-0.88	-0.54	-0.73	-0.70	0.94	-0.56	-0.13	-0.70	-0.88	-0.74	-0.45	-0.44	0.02	1.11	2.79	0.14	0.53	-0.31	0.79	-0.67
Greenland Shelf/Slope		0.57	0.72	-0.45	-1.96	-0.14	-1.94	1.66	1.14	1.16	0.21	0.65	-0.95	0.05	-0.79	-0.91	-0.98	-0.81	0.79	-1.67	-1.76
Calanus hyperboreus																					
Labrador Shelf/Slope		-0.79	-0.21	1.22	1.20	0.26	-0.80	0.13	-0.73	-1.02	-0.29	-0.36	2.17	-1.29	-0.04	-0.81	1.37	0.27	-0.59	1.19	-1.63
Labrador bassin		0.20	-0.02	-0.38	-0.96	-0.80	0.51	0.03	-1.30	-1.35	0.83	0.45	0.15	2.85	-0.15	0.44	-0.50	0.17	-0.58	1.93	-0.60
Greenland Shelf/Slope		-0.97	1.54	-1.20	-1.88	-0.15	-0.56	1.29	0.00	-1.30	-0.23	-0.32	1.25	-0.22	-1.22	1.26	0.82	1.28	1.33	-0.50	0.21
Oithona spp.																					
Labrador Shelf/Slope		-0.65	-0.55	-0.62	-0.77	0.28	-0.12	-0.20	0.10	1.52	-0.37	0.04	2.50	-1.52	0.52	-1.05	0.88	1.84	0.96	1.47	-1.22
Labrador bassin		2.66	-0.81	-0.62	0.17	-0.01	-0.65	-0.47	0.61	2.03	-0.72	-0.34	0.03	-0.72	-0.33	-0.62	-0.22	-0.46	-0.42	-0.67	-0.70
Greenland Shelf/Slope		0.86	-1.40	-0.62	-1.54	1.77	-0.85	0.14	0.78	1.50	-0.95	0.36	-0.77	-1.12	-0.45	1.00	-0.26	-1.00	5.12	0.02	0.05
Euphausids																					
Labrador Shelf/Slope		-0.99	-0.70	1.03	-0.12	-0.69	-0.55	-0.48	2.43	-0.19	-0.81	0.62	-0.70	-1.09	1.62	0.26	0.34	-0.53	0.34	0.90	-0.93
Labrador bassin		-0.31	-0.66	-0.88	-0.24	0.77	1.38	-0.25	2.90	-0.99	-0.76	-0.32	0.48	-0.60	0.32	-0.42	-0.40	0.19	1.73	1.36	-1.03
Greenland Shelf/Slope		-0.51	-0.85	-0.65	-0.95	0.15	2.73	-0.47	-0.53	-0.70	-0.78	-0.47	0.13	1.80	0.20	-0.17	0.13	0.03	1.74	0.20	0.02
Gastropods																					
Labrador Shelf/Slope		-0.19	-1.04	-0.92	0.38	1.18	-0.58	0.25	-0.89	1.29	-0.92	0.21	2.17	-0.95	-0.41	-0.76	1.18	0.53	0.82	2.42	-0.94
Labrador bassin		-0.38	-0.35	-0.42	-0.11	-0.25	-0.36	-0.30	0.05	3.52	-0.42	-0.37	-0.42	-0.43	-0.41	-0.31	0.96	-0.02	-0.18	-0.16	-0.44
Greenland Shelf/Slope		1.95	-0.56	-0.54	-0.57	-0.34	-0.52	-0.49	0.11	2.75	-0.42	0.35	-0.55	-0.54	-0.50	-0.38	-0.31	-0.42	0.65	-0.43	-0.49

-3 -2 -1 0 1 2 3

Figure 23. Normalised anomaly of physical, chemical and biological in-situ measurements on the AR7W line between 1994 and 2013.